ORNL-5152
UC-35

Contract No. W-7405-eng-26

Emergency Technology Section
HEALTH PHYSICS DIVISION

TRANSIENT RESPONSE OF NUCLEAR POWER PLANT CABLES TO HIGH-ALTITUDE NUCLEAR ELECTROMAGNETIC PULSE (EMP)

P. R. Barnes
J. H. Marable

MAY 1976

OAK RIDGE NATIONAL LABORATORY
Oak Ridge, Tennessee 37830
operated by
UNION CARBIDE CORPORATION
for the
ENERGY RESEARCH AND DEVELOPMENT ADMINISTRATION

CONTENTS

TRANSIENT RESPONSE OF NUCLEAR POWER PLANT CABLES TO HIGH-ALTITUDE NUCLEAR ELECTROMAGNETIC PULSE (EMP)

P. R. Barnes
J. H. Marable

ABSTRACT

The electromagnetic pulse (EMP) produced by a high-altitude nuclear detonation consists of a transient pulse of high intensity electromagnetic fields. These intense fields induce current and voltage transients in electrical conductors. Although nuclear power plant cables are not directly exposed to these fields, attenuated fields will couple some EMP energy to these cables. In this study, theoretical and experimental techniques have been used to determine the EMP surges induced in several types of cables typically used in nuclear plants. It was found that unshielded lines such as power cables within the plant building may have EMP surge peaks as high as 88 kV induced between the cables and the earth. Shielded cables such as coaxial cables will have EMP surge peaks in the tens of volts. Cables located in electromagnetically tight conduit will have only small EMP-induced transients on the order of several millivolts or less.

---

1. INTRODUCTION

1.1 Purpose and Content

This report has been prepared to give examples of the surge currents and voltages induced in idealized nuclear power plant circuits by the electromagnetic pulse (EMP) from high-altitude nuclear detonations. It is hoped that this information will be useful to designers and engineers concerned with nuclear safety. Several types of cables used in nuclear plant control, instrumentation, and power circuits are considered. The shielding effects of conduits and cable trays are also discussed. The surges induced in off-site power lines are not presented here, since they have been considered in a previous study.[1]

A preliminary analysis of the EMP effects on modern nuclear power plants is in progress at the Oak Ridge National Laboratory. The results of this report will be applied to that analysis. The examples of the EMP-induced cable transients presented in this report are severe, yet

moderately realistic, cases. These transients should be applicable for a conservative analysis of the EMP effects on nuclear power plants.

1.2 High-Altitude EMP

High-altitude EMP is produced by a nuclear detonation at an altitude near or above 50 km. The gamma radiation from the nuclear burst interacts with the atmosphere to generate a Compton electron current. This Compton current is the source of the intense electromagnetic pulse. Due to the large area of the source current, high-altitude EMP can cover a large portion of the country which is completely free from the other nuclear weapon effects. Typical areas of coverage for a megaton-range weapon, detonated at a height of burst of 100 and 400 km, are shown in Fig. 1.1. As shown, most of the United States can be covered by a single exoatmospheric burst.

The EMP fields are very intense. The amplitude of the electric field pulse is on the order of 50 kV/m. The time history of an EMP is characterized by a very short rise time of about 10 nsec and an exponential-type decay with a time constant on the order of 200 nsec. A double exponential is often used to describe the EMP waveform. An example of a double-exponential EMP time history is shown in Fig. 1.2. The double-exponential waveform shown in Fig. 1.2 is given by

$$E(t) = E_o(e^{-\alpha t} - e^{-\beta t}) \quad , \tag{1.1}$$

where

$$E_o = 53 \text{ kV/m} \quad ,$$
$$\alpha = 5 \times 10^6 \text{ sec}^{-1} \quad ,$$
$$\beta = 5 \times 10^8 \text{ sec}^{-1} \quad .$$

Equation (1.1) is a convenient representation of the EMP electric field. It has been used to compute the EMP surges described later in this report.

1.3 Shielding Effects of the Plant Buildings

The control, auxiliary, and reactor buildings of a nuclear power plant are reinforced concrete structures. Substantial electromagnetic shielding is provided to the center volume of a reinforced concrete building by the steel reinforcing bars. However, the shielding

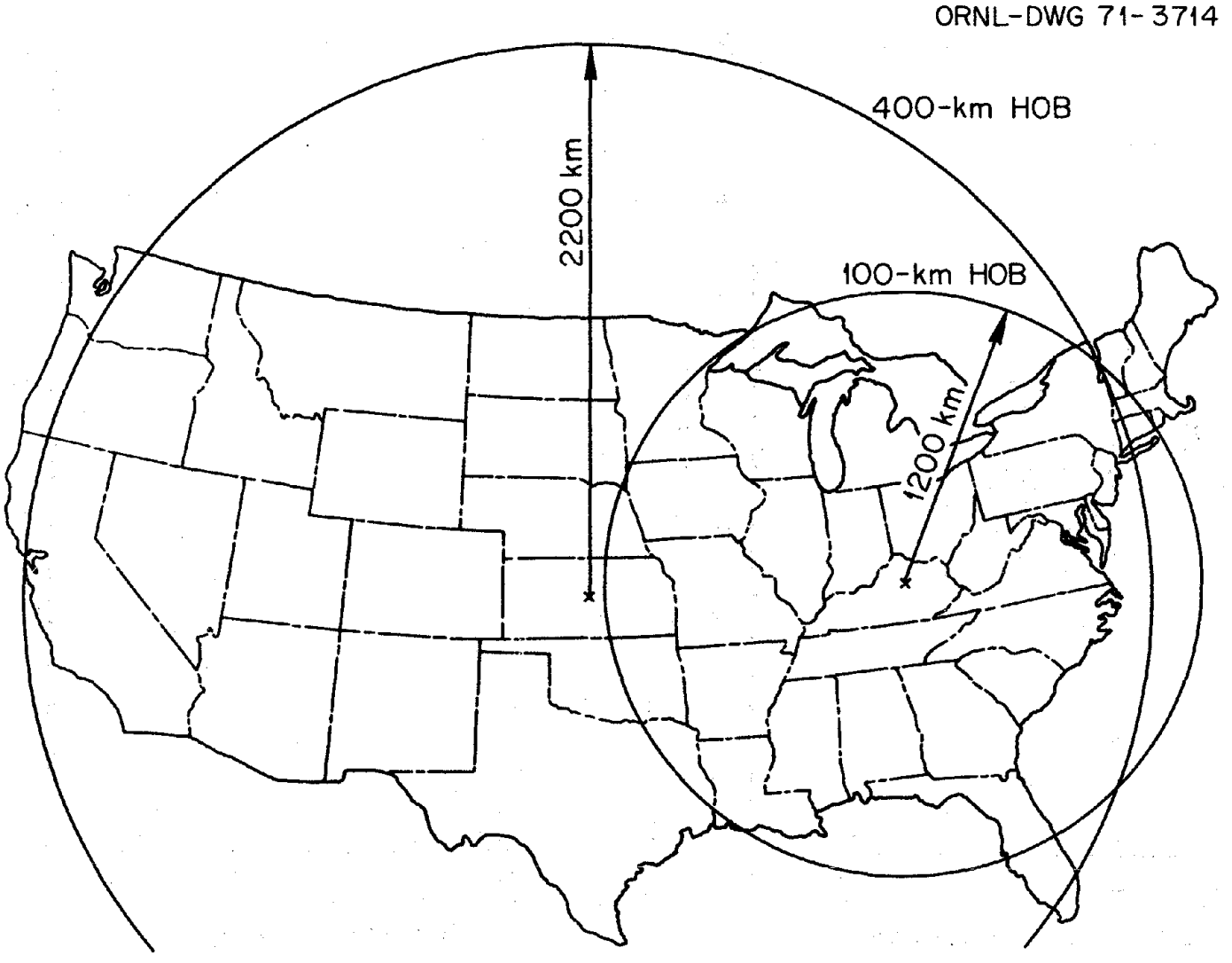

Fig. 1.1. Area of Coverage of EMP from High-Altitude Detonations.

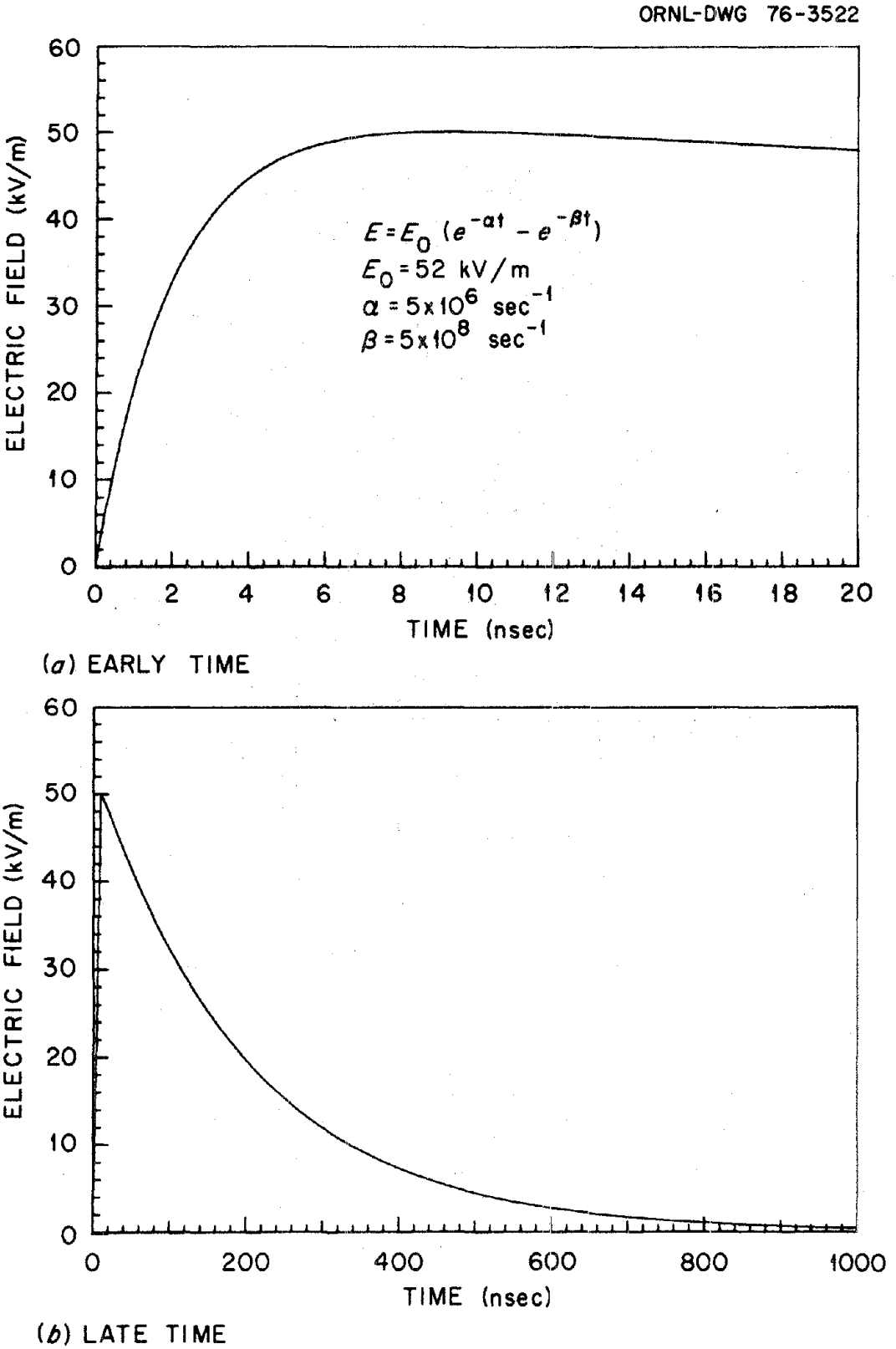

Fig. 1.2. Double-Exponential Waveform Used to Represent the EMP Electric Field Time History.

effectiveness of the reinforcing bars decreases sharply near the exterior walls of the building.

The EMP electric and magnetic field shielding effectiveness, S_E and S_H respectively, are defined in terms of the peak exterior and interior fields by

$$S_E = 20 \log_{10} \frac{|E_e(t)|_{peak}}{|E_i(t)|_{peak}} \quad \text{dB} \qquad (1.2)$$

and

$$S_H = 20 \log_{10} \frac{|H_e(t)|_{peak}}{|H_i(t)|_{peak}} \quad \text{dB} \quad , \qquad (1.3)$$

where E_e and E_i are the exterior and interior electric fields respectively, and H_e and H_i are the exterior and interior magnetic fields respectively. For a thick conducting sheet, the electric and magnetic shielding effectiveness are equal.[2]

The electric field shielding effectiveness for the Sequoyah nuclear plant control room was experimentally determined by ORNL personnel for FM and AM broadcast band frequencies. Existing radio signals and standard radio frequency electric field-measuring equipment were used. At FM frequencies we found that $S_E \approx 20$ dB and at AM frequencies $S_E \approx 25$ dB. The Sequoyah control room is located on the top floor in the control building.

The magnetic shielding effectiveness of reinforced concrete has been considered by Bell Laboratories.[2] For 1-in., double-course rebar with 6-in. spacing, the magnetic shielding effectiveness at 100 kHz ranges from 17 dB near the wall to over 43 dB at the center of a large building. The magnetic shielding effectiveness of rebar decreases as the frequency is decreased.

At this point, we make some assumptions that will both simplify the analysis and result in conservative EMP surge estimates. We assume that the cables that we are considering are routed near the exterior walls or on the top floor of the building. This minimizes the shielding effectiveness of the building. Furthermore, we assume that the shielding

effectiveness is not a function of frequency and that $S_E = S_M = 20$ dB. These simplifications make the EMP coupling problem more tractable and result in more energy coupled to the cables.

2. COUPLING TO THE UNSHIELDED CABLES

2.1 Introduction

There are numerous unshielded power and control cables in a nuclear power plant. Several voltage levels are used to transmit power and control signals. Large motors operate at several kilovolts ac, whereas small motors and other equipment typically operate at 480 Vac or 240 Vac. Instrumentation and control equipment typically use 120 Vac for power. Instrument and control signals are normally 120 V or lower and may be ac or dc voltages.

These cables will be subjected to electromagnetic fields that penetrate the building walls. As discussed in Section 1, a slightly more than "worst case" electromagnetic environment can be specified by assuming an electric and magnetic field shielding effectiveness equal to 20 dB for all the frequencies of interest. This assumption applies to cables that are installed near the exterior walls. The surges induced on cables which do not run near the exterior walls or the top of the building will be about one-tenth those calculated in this report.

The EMP environment we have assumed for the cables is an electromagnetic plane wave pulse with the double-exponential time history described by Eq. (1.1). Due to the attenuation of the building, the amplitude of the internal electric field is one-tenth that given by Eq. (1.1). Since we have assumed that the shielding effectiveness of the electric and magnetic fields are equal, the internal magnetic field is by

$$H_i = \frac{E_i}{Z} \quad , \tag{2.1}$$

where Z is the free-space wave impedance approximately equal to 120π ohms, and E_i is the internal electric field.

2.2 Coupling Analysis

A typical circuit employing an unshielded cable is shown in Fig. 2.1a. The cable is connected to a load which may be an electronic system, a motor, a solenoid, a relay, etc. The load has an input impedance Z_e. The cable is driven by a voltage source V_s which has a source impedance Z_s. The source may be an ac power or signal transformer, an isolation

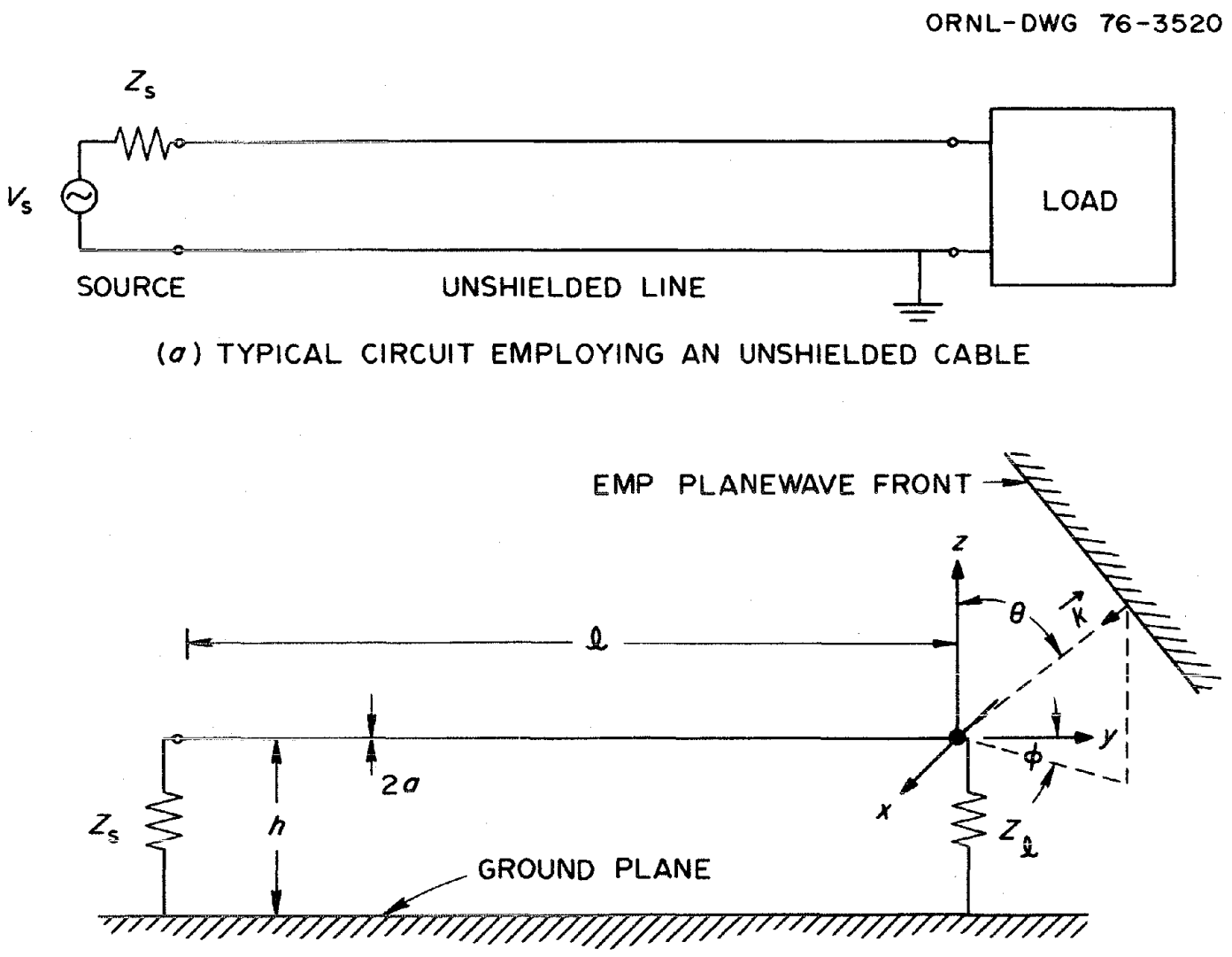

Fig. 2.1. Unshielded Cable and Transmission Line Model for the Analysis of EMP Surges.

or bistable amplifier, etc. The ground return line is typically grounded at the load end of the cable as shown.

Unshielded cables are good receiving antennas for EMP. Voltage surges are developed between each wire and the earth ground which forms the return conductor for the common mode currents. The earth and each wire in the cable forms a transmission line as shown in Fig. 2.1b. The transmission line model for EMP analysis has been used in previous studies.[1] Scattering theory is used to compute the current induced by the incident and ground-reflected EMP waves. This current is used as the source current in the transmission line equations.

Many of the unshielded lines in a nuclear plant are connected to a transformer or a high-impedance circuit. To simplify the analysis of the unshielded line, we set $Z_S = \infty$ to represent a high source impedance. The line itself is idealized to a straight wire of radius a, located h meters above the earth. The ground mat is assumed to be covered with several meters of earth, such that the earth forms the ground return line for the frequencies of interest (10 MHz to 0.1 MHz). To achieve the maximum coupling, we have assumed that the grounded and ungrounded lines are not run together. The induced current in cables which contain both lines is reduced by about a factor of two.

The incident EMP plane wave and the induced current are shown in Fig. 2.1b. The incident direction of the EMP is determined by the angles ϕ and θ associated with the propagation vector $\vec{k}$, as shown. The direction of the electric field is then specified by the angle ψ between the electric field vector $\vec{E}$ and the vertical plane containing the propagation vector $\vec{k}$. The angle between $\vec{E}$ and the horizontal is given by $\sin^{-1}(\sin\theta \cos\psi)$. For detonations over the continental United States, the angle between $\vec{E}$ and the horizontal is always less than 30°, so θ and ψ are restricted to the range $\sin\theta \cos\psi \leq 0.5$.

2.3 Surges on Unshielded Lines

The calculated EMP surges induced on the unshielded lines that are near the exterior walls or the top of the plant building are shown in Appendix A. Two EMP wave incident cases have been considered. One case is broadside incidence with the electric field horizontally polarized

($\theta = 80^o$, $\psi = 90^o$, $\phi = 90^o$), and the other is along-the-line incidence with the angle between the electric field vector and the horizontal equal to 29.5^o, i.e., ($\theta = 80^o$, $\psi = 60^o$, $\phi = 180^o$). The EMP electric field time history used to compute the surges is given by Eq. (1.1) with $\alpha = 5 \times 10^6$ sec^{-1}, $\beta = 5 \times 10^8$ sec^{-1}, and $E_o = 5.3$ kV/m. Three lengths of lines have been considered: semi-infinite, 160 m, and 20 m. All lines have a radius of 3.25 mm and are located 10 m above the earth. The finite length lines are terminated at $y = -\ell$ (Fig. 2.1b) by an open circuit.

The largest response for a long line is obtained by the incident wave traveling along the line in the positive y direction ($\phi = 180^o$), whereas the largest response for a short line is obtained by broadside incidence ($\phi = 90^o$). The open circuit voltage and short circuit current surges induced on a 160 m line with $\theta = 80^o$, $\psi = 60^o$, and $\phi = 180^o$ are shown as a linear function of time in Figs. 2.2 and 2.3. The voltage reaches a peak of about 88 kV after 35 nsec. The rise time from 10-90% is 20 nsec, and the rate of rise is 4MV/μsec. The late time voltage response is a damped oscillation with a dominant frequency of about 625 kHz. The current surge has a peak of near 165 A and a late time oscillating frequency of 416 kHz.

The open circuit voltage and short circuit current induced on a 20 m line for $\theta = 80^o$, $\psi = 90^o$, and $\phi = 90^o$ are shown in Figs. 2.4 and 2.5. The voltage surge has a peak of near 26 kV and a 10-90% rise time of 8 nsec. The rate of rise is 1.6 MV/μsec. The dominant late time oscillation frequency is about 5 MHz. The current surge has a peak of 52 A and a late time oscillation frequency of near 3.6 MHz.

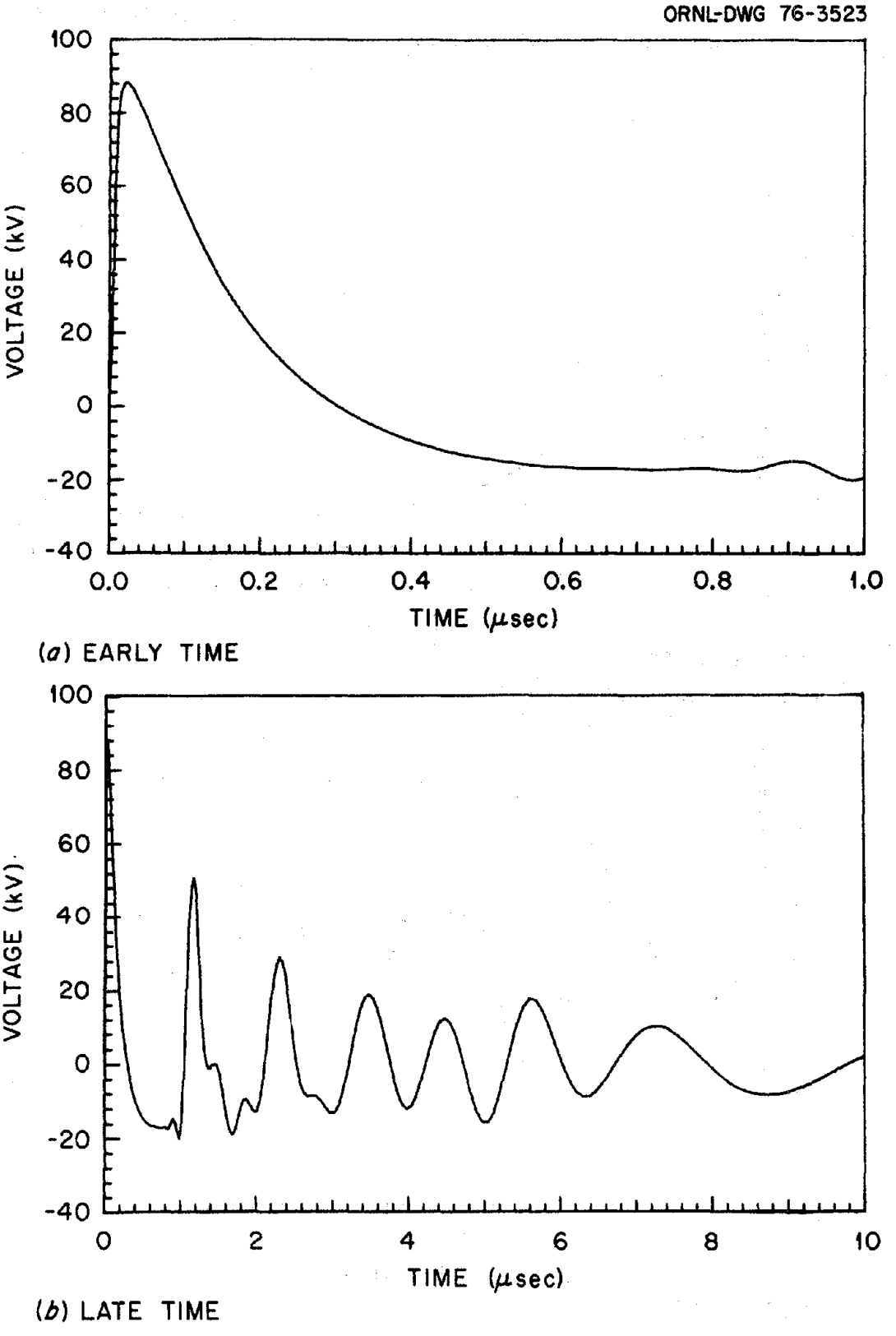

Fig. 2.2. The Open Circuit Voltage Induced on a 160 m Unshielded Line 10 m Above the Earth by the Representative EMP with $\theta = 80^{o}$, $\psi = 60^{o}$, and $\phi = 180^{o}$.

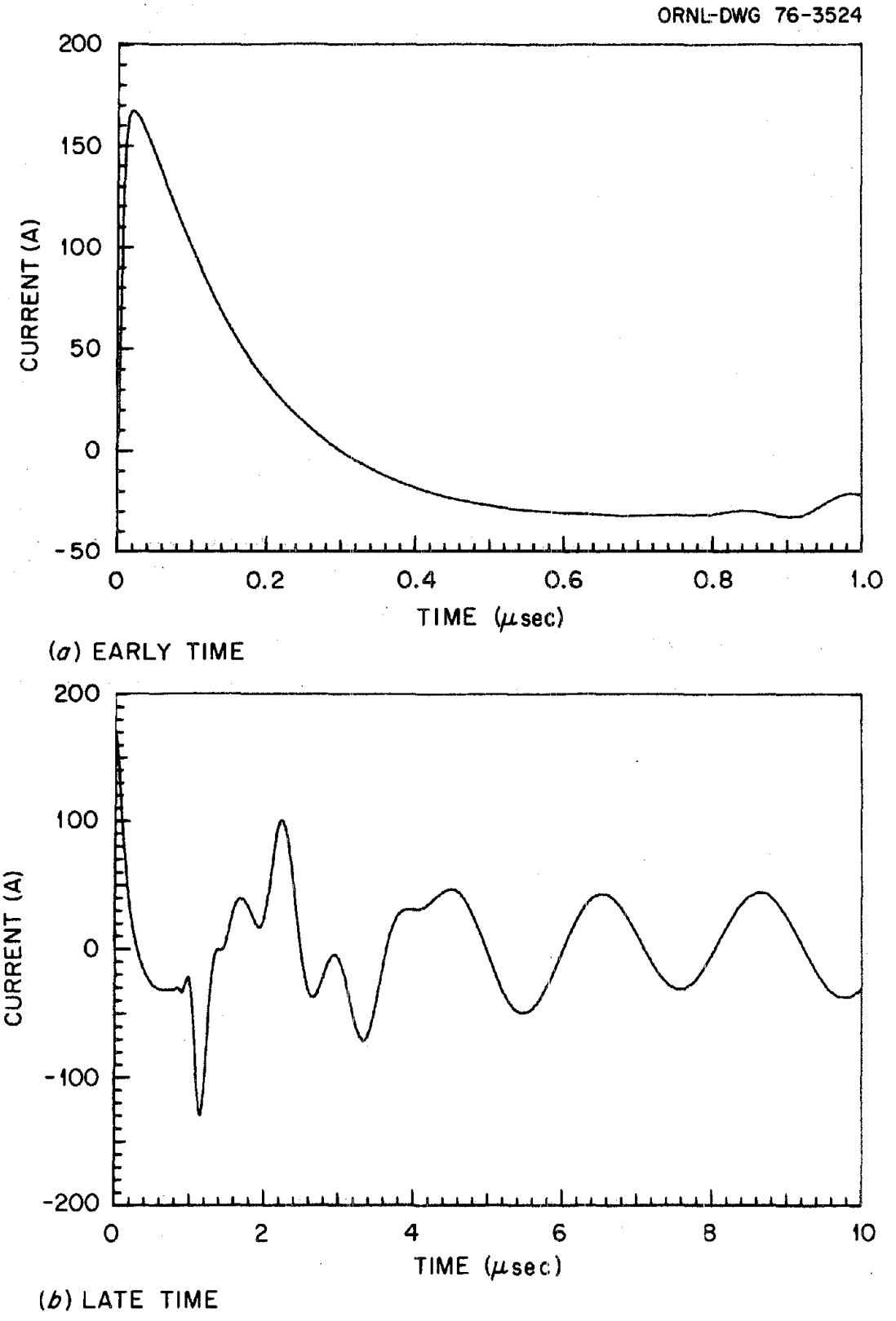

Fig. 2.3. The Short Circuit Current Induced on a 160 m Unshielded Line 10 m Above the Earth by the Representative EMP with $\theta = 80^{o}$, $\psi = 60^{o}$, and $\phi = 180^{o}$.

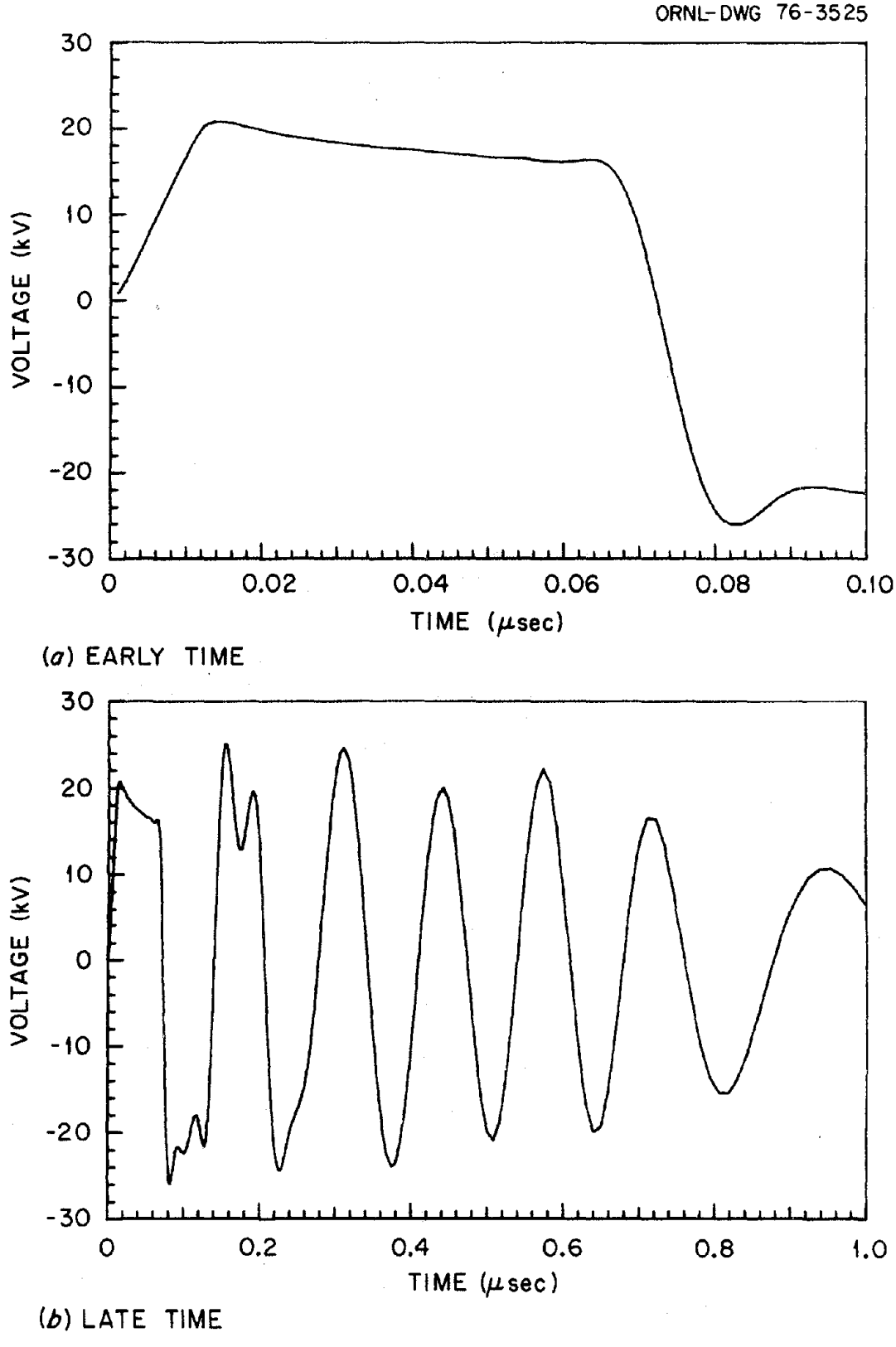

Fig. 2.4. The Open Circuit Voltage Induced on a 20 m Unshielded Line 10 m Above the Earth by the Representative EMP with $\theta = 80^{\circ}$, $\psi = 90^{\circ}$, and $\phi = 90^{\circ}$.

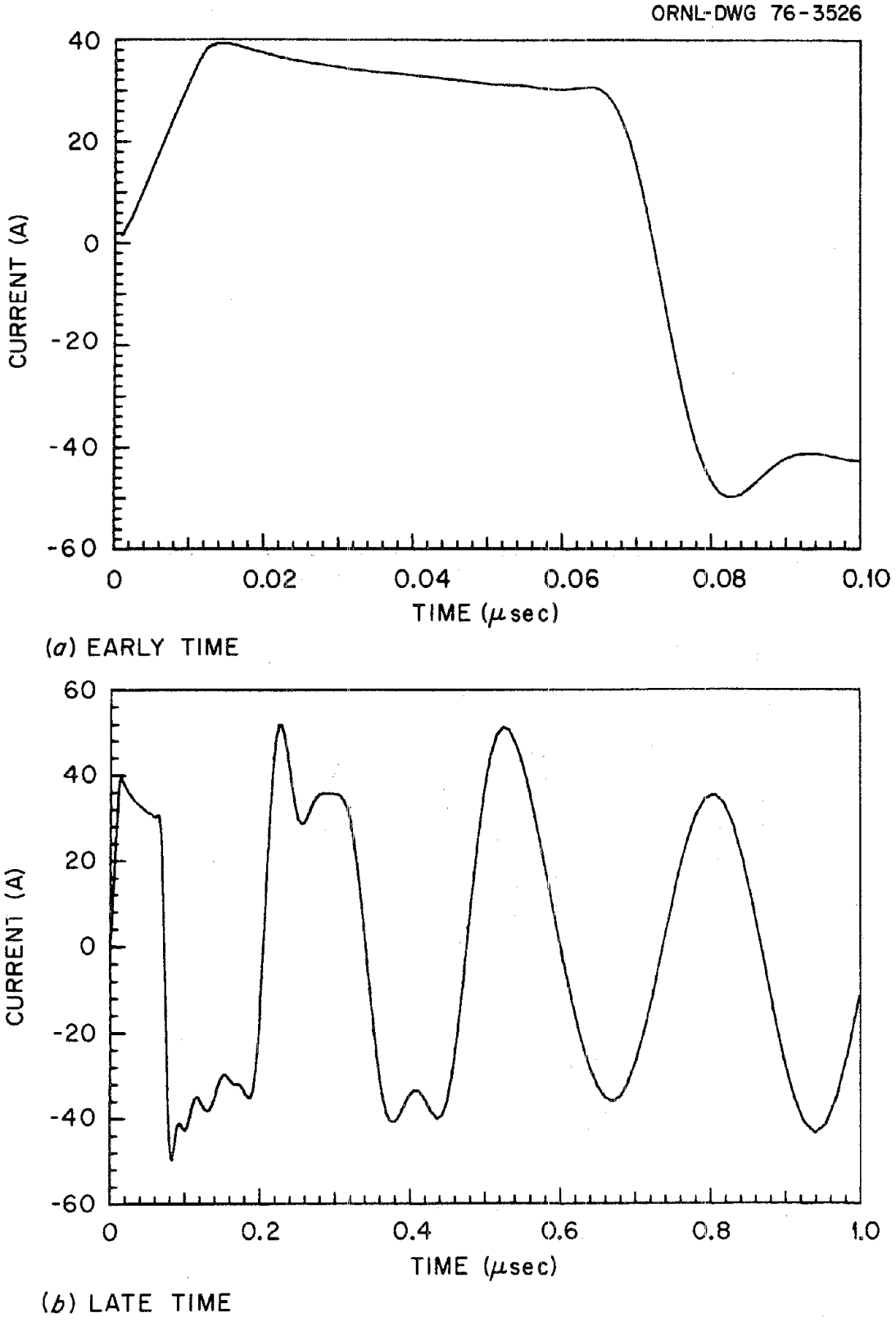

Fig. 2.5. The Short Circuit Current Induced on a 20 m Unshielded Line 10 m Above the Earth by the Representative EMP with $\theta = 80^{o}$, $\psi = 90^{o}$, and $\phi = 90^{o}$.

3. COUPLING TO SHIELDED CABLES

3.1 Instrumentation and Control Cables

Nuclear power plant instrumentation and control cables are well shielded to prevent electromagnetic interference. General Electric's boiling water reactor (BWR) plants employ RG-59B or similar coaxial cables to transmit power range nuclear instrumentation signals. Westinghouse pressurized water reactor (PWR) plants employ RG-11 triaxial cables to connect the power range nuclear detectors to the nuclear instrumentation equipment. Cable shields are normally grounded at the equipment end of the cables. Both BWR and PWR plants employ ferrous conduit for additional protection of nuclear instrumentation sensor cables.

Shielded, twisted-pair cables are used extensively in instrumentation and control circuits. This type of cable contains one or more internal twisted-pairs of wires and an external braided cable shield. Shielded, twisted-pair cables are normally placed in cable trays. Shielded, twisted-pair sensor cables are normally grounded at the equipment end of the cable.

3.2 Transfer Impedance and Admittance

The transfer impedance Z_T and the transfer admittance Y_T are important properties of the cable shield. The transfer impedance relates the distributed internal-voltage source to the shield current and is defined by[3]

$$Z_T = \frac{1}{I_o} \left. \frac{dV}{dz} \right|_{I=0} , \tag{3.1}$$

where I_o is the shield current, dV/dz is the internal voltage change per unit length along the cable, and I is the internal current.

The transfer admittance relates the internal current to the shield voltage and is defined by[3]

$$Y_T = \frac{1}{V_o} \left. \frac{dI}{dz} \right|_{V=0} , \tag{3.2}$$

where V_o is the voltage between the shield and the ground plane, and dI/dz is the current change per unit length flowing in the internal conductor.

For metal tubular shields with no apertures, the transfer admittance is equal to zero. For braided shields, the transfer admittance contains

a mutual capacitance term that accounts for the capacitive coupling between the internal conductors and the ground plane.

3.3 Open Circuit Voltage and Short Circuit Current

To accurately compute the open circuit voltage induced between the cable shield and the internal conductor, we shall employ both an early time and a late time model. In the early time model, the cable is idealized to a semi-infinite cable, as shown in Fig. 3.1a. The shield of the cable is terminated in an impedance Z_{oe}, as shown. The induced open circuit voltage is given by[3]

$$V_{oc} = \frac{I_o}{(\gamma - jk)} (Z_T - Z_o Z_{oe} Y_T) \quad , \tag{3.3}$$

where Z_o is the characteristic impedance of the cable, Z_{oe} is the characteristic impedance of the shield and the ground plane, $jk = s/c$ where s is the Laplace transform variable and c is the speed of light approximately equal to 3×10^8 m/sec, and γ is the propagation factor approximately equal to s/u where u is the propagation speed of the cable. For most braided cables, $|Z_T| >> Z_o Z_{oe} |Y_T|$ (Ref. 3).

Most of the shielded cables in a nuclear plant are grounded at the equipment end of the cable. The open circuit voltage as a function of s for a grounded shield cable is given approximately by

$$V_{oc} = \frac{I_s c Z_T}{s (\sqrt{E_r} - 1)} \quad , \tag{3.4}$$

where the electric coupling has been neglected and E_r is the dielectric constant of the insulation between the internal conductors and the shield. The dielectric constant is related to the propagation speed of the cable by

$$u \simeq \frac{c}{\sqrt{E_r}} \quad . \tag{3.5}$$

ORNL-DWG 76-3521

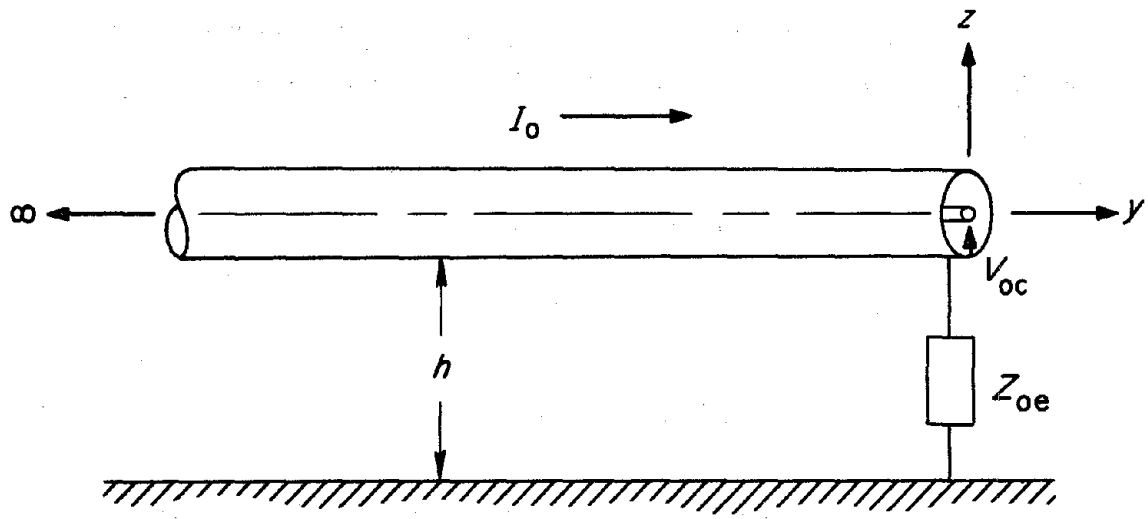

(*a*) SEMI-INFINITE SHIELDED CABLE

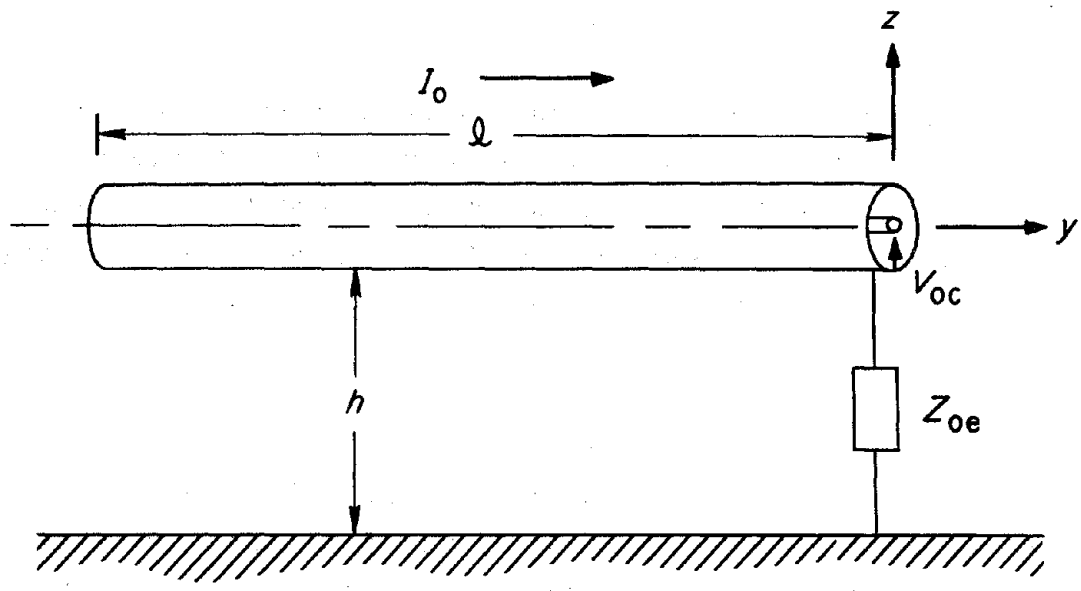

(*b*) FINITE LENGTH SHIELDED CABLE

Fig. 3.1. Models for the Analysis of Shielded Cables.

The value of u is about 1.98 m/sec for many shielded cables used in nuclear plants, such as RG-11/u and RG-59B coaxial and triaxial cables.

The solution for the semi-infinite cable is the same as that for the finite cable for time t in the range $0 \leq t \leq t_o$, where t_o is the time that the end reflection affects the solution. The time t_o is given by

$$t_o = \frac{\ell}{c} (1 - \cos \gamma) \quad , \tag{3.6}$$

where

$$\gamma = 180^o - \cos^{-1} (\sin \theta \cos \phi) \quad . \tag{3.7}$$

For $0 \leq t \leq t_{oi}$, where t_{oi} is computed by Eq. (3.6) with u substituted for c, the impedance looking into the cable is Z_o. The value of t_{oi} is larger than t_o, thus the short circuit current for $0 \leq t \leq t_o$ is

$$I_{sc} = \frac{V_{oc}}{Z_o} \quad . \tag{3.8}$$

The source impedance for many shielded cables is very large at the EMP frequencies of interest (0.01-100 MHz). For late times, $t > t_o$, the shield cable can be modeled as a finite cable of length ℓ, open-circuited at the source end as shown in Fig. 3.1b. The open circuit voltage is given, for $t >> \ell/c$, by[3]

$$V_{oc} \simeq I_o Z_T \ell \quad . \tag{3.9}$$

For times $t_o < t < 10\ell/c$, the magnitude of the induced voltage is bounded by Eq. (3.9), since the current is not uniform over the length of the cable. If a cosine current distribution ($I_o \cos (\pi z/2\ell)$) is assumed, then Eq. (3.9) gives a value too large by 36%. Also, Eq. (3.9) does not take into account the internal cable reflections, and the small amount of electric coupling through the shield has been neglected.

The short circuit current is given by

$$I_{sc} = \frac{V_{oc}}{Z_i} \quad , \tag{3.10}$$

where Z_i is the impedance between the internal conductors and the shield. The cable impedance is

$$Z_i = Z_o \left[\frac{1 + e^{-2s\ell/u}}{1 - e^{2s\ell/u}} \right] \quad . \tag{3.11}$$

3.4 Shielding Effectiveness

The shielding effectiveness S is a commonly used measure of the quality of a cable shield. The shielding effectiveness S is defined by

$$S = 20 \log_{10} \frac{I_o}{I} \quad , \tag{3.12}$$

where I_o is the cable shield current, and I is the current in the internal conductor. The shielding effectiveness depends on the length of the cable and the cable terminations. The shielding effectiveness decreases as the cable length increases. The shielding effectiveness S_2 of a cable of length ℓ_2 is given by[4]

$$S_2 = S_1 - 20 \log_{10} \frac{\ell_2}{\ell_1} \quad , \tag{3.13}$$

where S_1 is the shielding effectiveness of the same type of cable with length ℓ_1 and $\ell_2 > \ell_1$. The shielding effectiveness can be calculated from the transfer and terminating impedances for frequencies with wavelengths much larger than ℓ by

$$S = 20 \log_{10} \left(\frac{Z_1 + Z_2}{\ell Z_T} \right) \quad , \tag{3.14}$$

where Z_1 and Z_2 are the terminated impedances at ends one and two, respectively.

The shielding effectiveness can be used to estimate the late-time, open circuit voltage and short circuit current responses. The ratio

of the shield and internal conductor currents as determined by a shielding effectiveness test is given by

$$S_t = \frac{I_{ot}}{I_t} = 10^{S/20} = \frac{2\ Z_o}{\ell_t\ Z_T} \quad , \tag{3.15}$$

where I_{ot} and I_t are the measured shield and internal currents, respectively, S is the shielding effectiveness as defined by Eq. (3.12), the cable is terminated at both ends by Z_o, and ℓ_t is the length of the tested cable.

The open circuit voltage is

$$V_{oc} = \frac{2\ I_o\ \ell\ Z_o}{\ell_t\ S_t} \quad , \tag{3.16}$$

and the short circuit current is given by Eq. (3.10).

In many shielding effectiveness tests, the shielding effectiveness is defined by the ratio of the maximum shield and internal currents.

$$S_m = \frac{i_o(t)\big|_{max}}{i(t)\big|_{max}} \quad . \tag{3.17}$$

The peak induced voltage can be estimated by

$$V_{oc}\Big|_{max} = \frac{2\ \ell\ Z_o\ i_{om}}{\ell_t\ S_m} \quad , \tag{3.18}$$

where i_{om} is the peak shield current.

3.5 Braided-Wire Cable Shields

Cables with braided-wire shields are commonly used in nuclear plant instrumentation and control systems. The transfer impedance for a braided shield contains a diffusion term that accounts for the finitely conducting shield and a mutual inductance term that accounts for the coupling through the apertures in the shield. The transfer impedance is given by

$$Z_T = \frac{R_o \sqrt{s\tau}}{\sinh (\sqrt{s\tau})} + sM \quad , \tag{3.19}$$

where τ is the diffusion time constant, R_o is the dc resistance of the shield per unit length, and M is the leakage inductance.

For RG-59B coaxial cable,[3] τ = 1.87 μsec, R_o = 8.1 mΩ/m, and M = 0.14 nH/m. For triaxial cables, i.e., double-shielded coaxial cables such as RG-11 triaxial, $R_o \simeq 4$ mΩ/m and $\tau \simeq 1.87$ μsec. The leakage inductance is significantly reduced by the extra shield to about 5 pH/m, as presented in Ref. 5.

The early-time open circuit voltage surges induced in RG-59B coaxial and RG-11 triaxial cables are shown in Fig. 3.2. Equation (3.4) has been used to calculate the voltages in Fig. 3.2. The semi-infinite model can be applied for the first 8 nsec to a finite cable, 160 m in length, subjected to an EMP with $\theta = 80^o$, $\psi = 60^o$, and $\phi = 180^o$.

The late-time surges valid for times much, much greater than 8 nsec is shown in Figs. 3.3 and 3.4 for an EMP with $\theta = 80^o$, $\psi = 60^o$, and $\phi = 180^o$. Waveforms for broadside incidence are shown in Appendix B. The late-time waveforms have been computed using Eq. (3.9). The early-time portion (0 to 8 nsec) of the waveforms shown in Figs. 3.3 and 3.4 are not necessarily accurate. The valid portion of the waveforms show that the peak open circuit voltage of the 160 m coaxial and triaxial cables are near 80 V and 44 V, respectively. For broadside incidence, the coaxial cable voltage peak is 36 V and the triaxial cable voltage peak is 17 V, as shown in Figs. B3 and B5 in Appendix B.

3.6 Shielded Twisted Pairs and Multiconductor Cables

The shielding effectiveness of a shielded cable can be increased by employing a twisted pair of internal conductors. At low frequencies below 5 kHz, the magnetic coupling reduction of a twisted pair is greater than 20 dB, whereas copper-braid shielding will provide practically none. Pulse tests on braided shield cables with both twisted pairs and single conductors indicate that the amplitude of the surge coupled to a shielded twisted pair is at least 20 dB below that of a shielded single conductor.[6] The surge in the twisted pair was measured from conductor

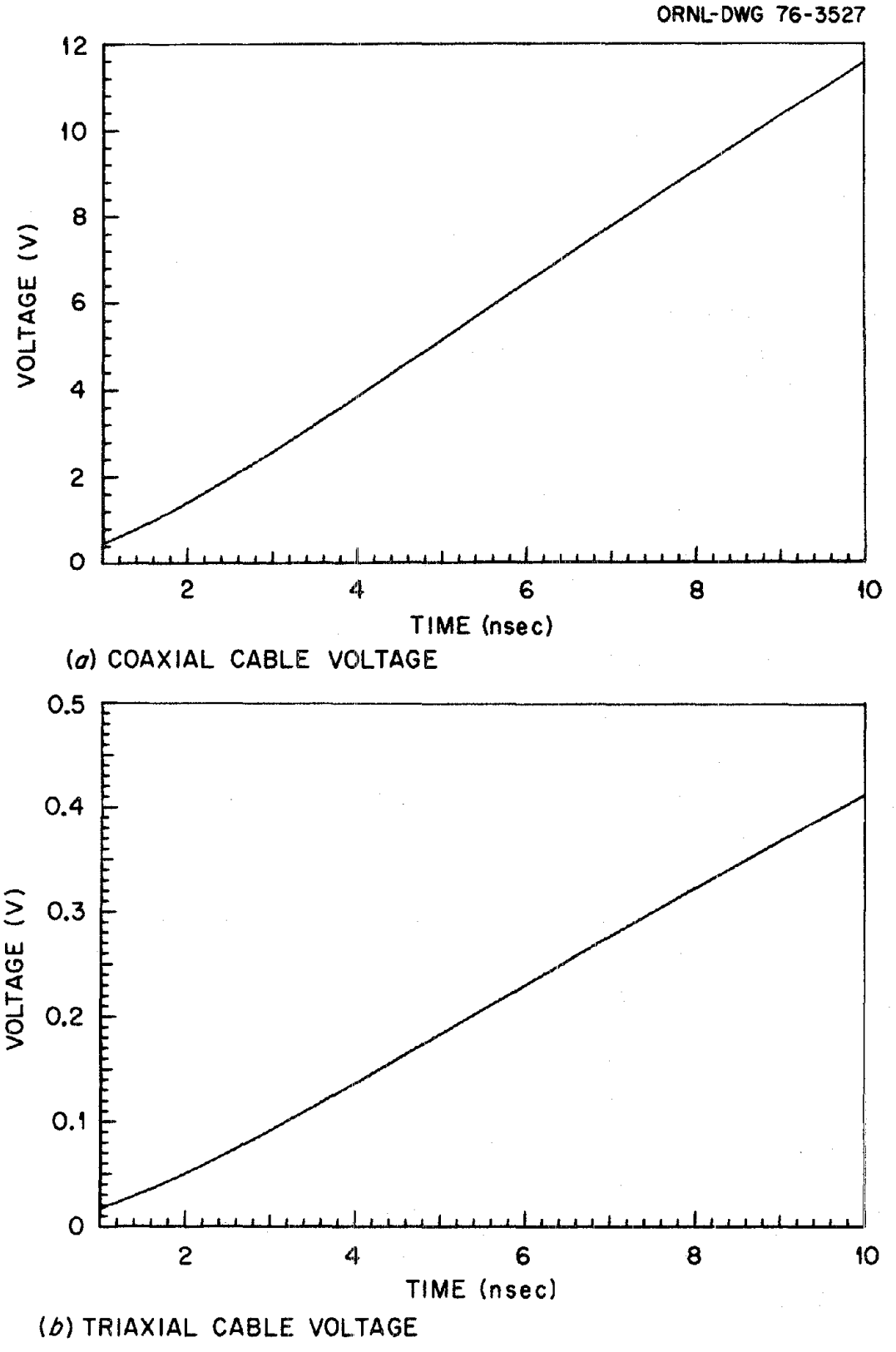

Fig. 3.2. Open Circuit Voltage Surges Induced in Semi-Infinite Cables Located 10 m Above the Earth by the Representative EMP with $\theta = 80^{\circ}$, $\psi = 60^{\circ}$, and $\phi = 180^{\circ}$.

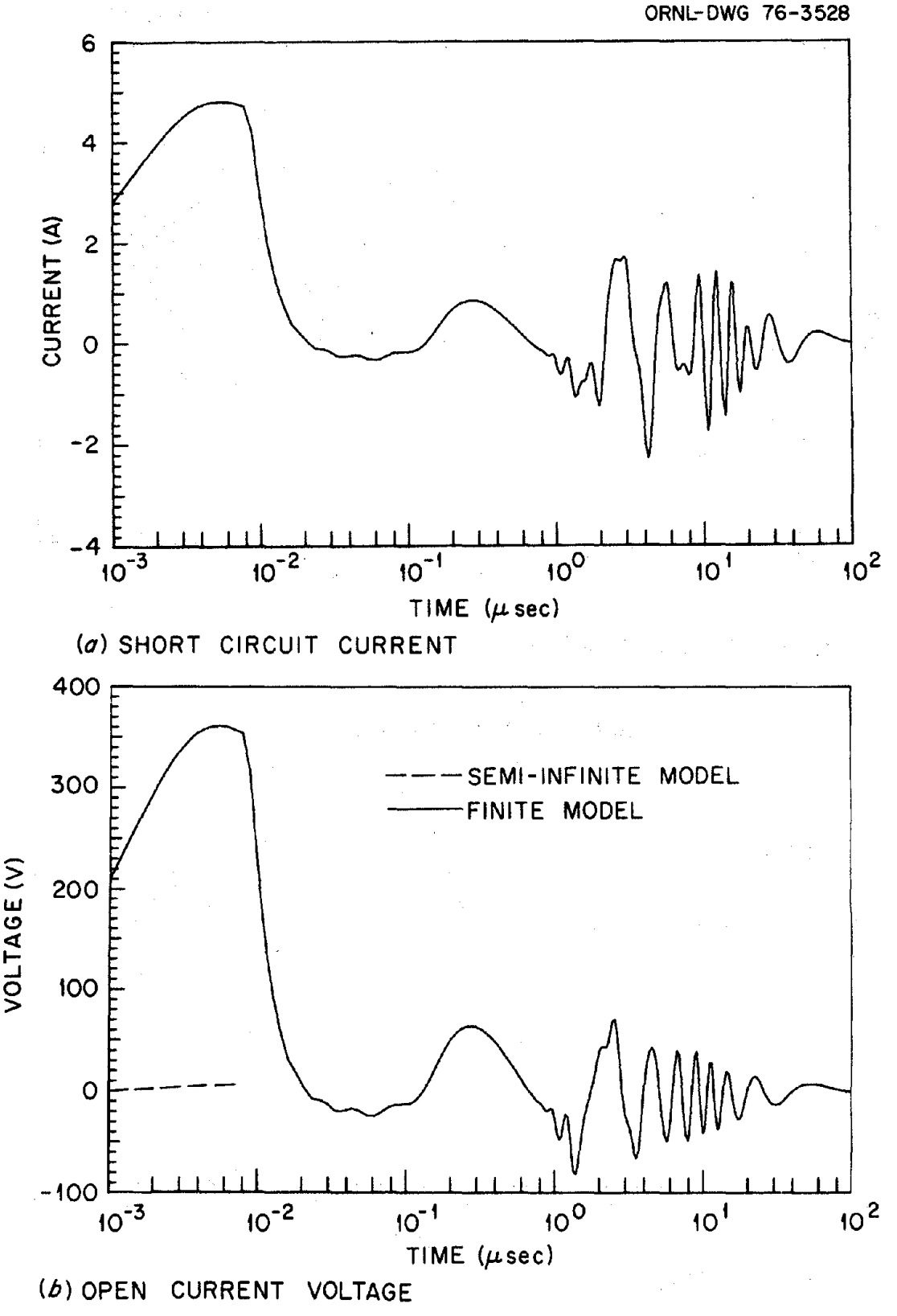

Fig. 3.3. Surges Induced in a 160 m Coaxial Cable Similar to RG-59B Located 10 m Above the Earth by the Representative EMP with $\theta = 80^{\circ}$, $\psi = 60^{\circ}$, and $\phi = 180^{\circ}$.

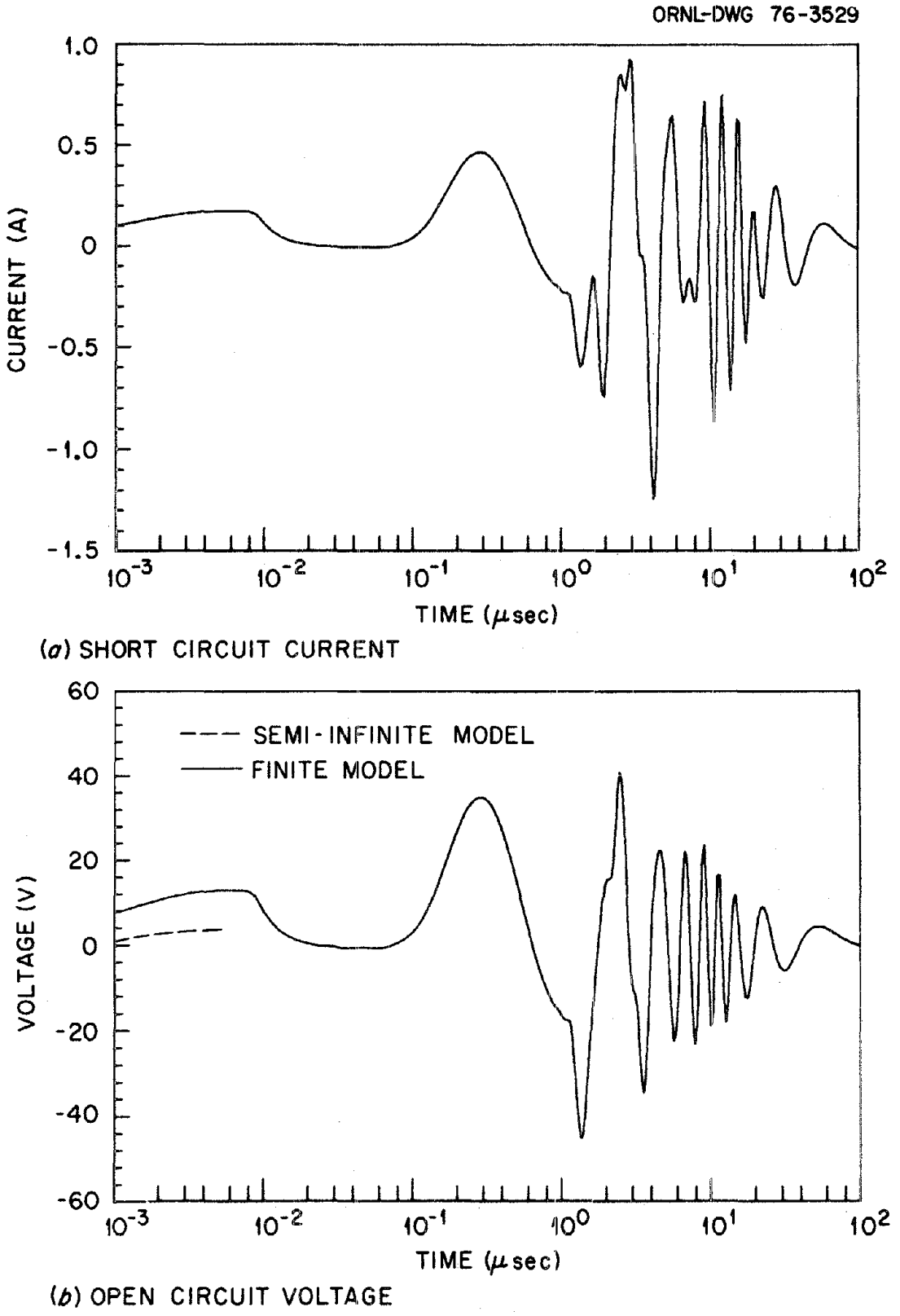

Fig. 3.4. Surges Induced in a 160 m Triaxial Cable Located 10 m Above the Earth by the Representative EMP with $\theta = 80^{\circ}$, $\psi = 60^{\circ}$, and $\phi = 180^{\circ}$.

to conductor, and the surge in the single conductor was measured from the conductor to the shield.

Pulse tests on shielded multiconductor cables indicate that the number of internal conductors is not an important factor in the magnitude of the induced surge on each conductor. Also, no consistent relationship was found between the magnitude of the surge on an inner conductor and the location of the conductor in the bundle.[6] For our purposes, it is sufficient to employ the transfer impedance of a shielded single-conductor cable for each conductor of a multiconductor cable.

3.7 Double-Grounded, Braided Shield Cables

A braided shield cable with its shield grounded at both ends forms a ground wire loop. This increases the magnetic coupling to the cable shield. For a 160 m cable located 10 m above the earth, the EMP-induced current peak for the double-grounded cable shield is over twice that of the single-grounded cable shield. The open circuit voltage surges induced between the inner conductor and the external shield are shown in Fig. 3.5. Comparing Figs. 3.5a with 3.3b, and 3.5b with 3.4b, we find that the peak late-time voltage in the coaxial cable is increased by 25% and the triaxial cable voltage is increased by 5%, due to the double grounding of the shield. Thus, double grounding the shield decreases the EMP shielding effectiveness of a coaxial cable by 12 dB and a triaxial cable by 6 dB.

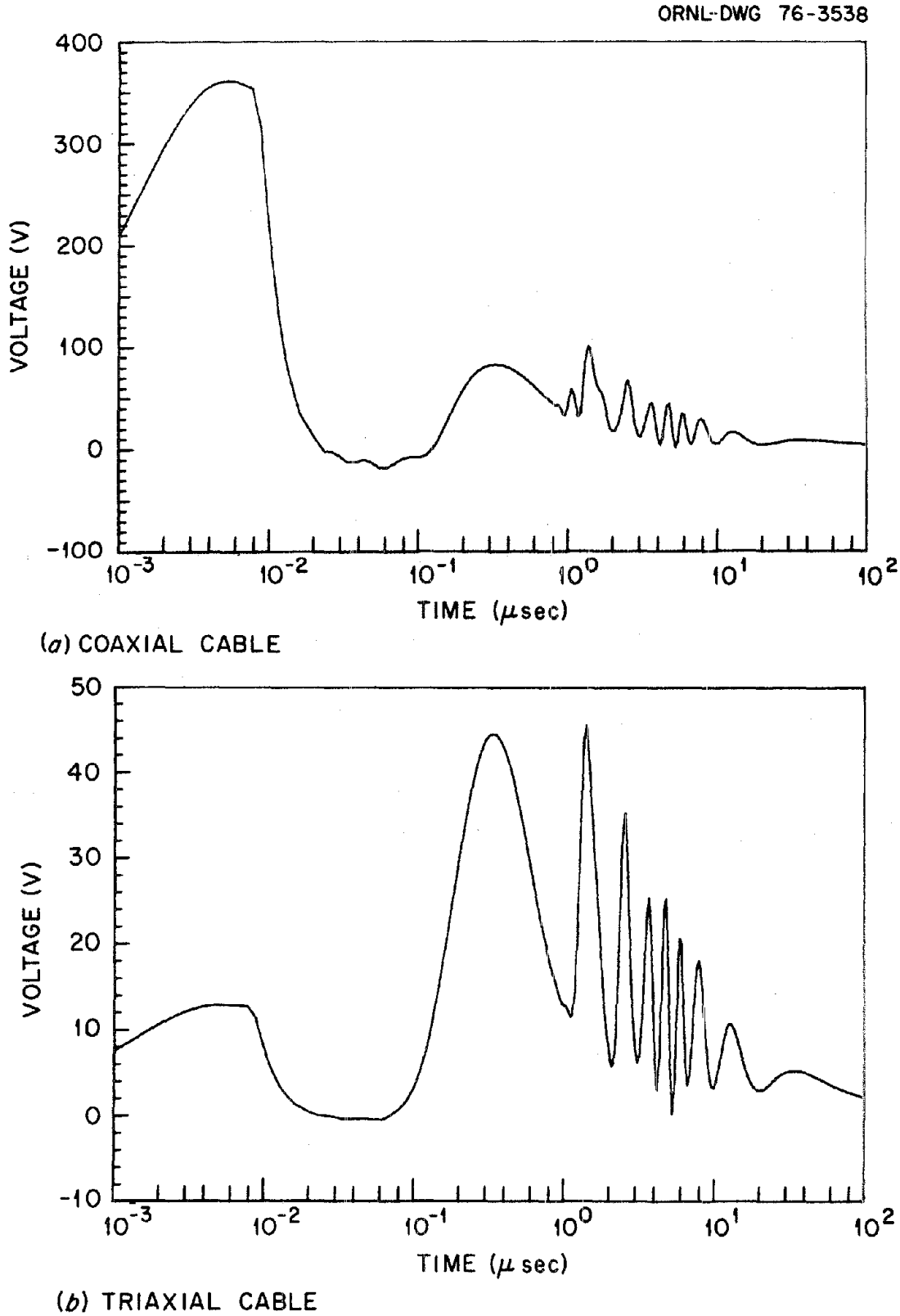

Fig. 3.5. Open Circuit Voltage Surges Induced in 160-m-Long Cables with Their Cable Shields Grounded at Both Ends and Located 10 m Above the Earth by the Representative EMP with $\theta = 80^{\circ}$, $\psi = 60^{\circ}$, and $\phi = 180^{\circ}$.

4. ADDITIONAL SHIELDING

4.1 Introduction

Additional shielding is provided to the plant cables by conduit, cable trays, and the building interior. Some cables such as the nuclear instrumentation cables are protected by conduits for the entire length of their cable paths. Other cables are routed through conduits in some sections of the building and are placed in cable trays for the remainder of their cable routes. Still other cables are run only in cable trays. Most of these cables are routed through the building interior where additional EMP shielding is provided by the building. In this section, we will estimate the effects of the additional shielding provided by the plant structures on the peak value of the EMP-induced cable surges.

4.2 Coupling through Conduit

Electromagnetic energy couples through the conduit system by the direct diffusion of the external signal through the conduit walls and by the leakage of signals through holes or flaws in the conduit. The diffusion process has many characteristics of a low-pass filter and only the low frequency signal couples to the internal cables. For most EMP pulses the conduit current will have decayed to a very low value before the diffusion signal rises to an appreciable magnitude.

The diffusion component of the transfer impedance for conduit is[3]

$$Z_T = \frac{R_o \sqrt{s\tau}}{\sinh \sqrt{s\tau}} \quad , \tag{4.1}$$

where for 2-in., standard galvanized, rigid steel conduit, R_o = 0.24 mΩ/m and τ = 57.7 msec.

The early-time current induced on a 160-m-long, 2-in. conduit located 10 m above the earth by the representative EMP with $\theta = 80^o$, $\psi = 80^o$, and $\phi = 180^o$ is shown in Fig. 4.1a. The conduit is grounded at both ends. The late-time current (not shown) is a damped oscillation with a dominant frequency near 500 kHz. The late-time current decays to near zero after 7 μsec.

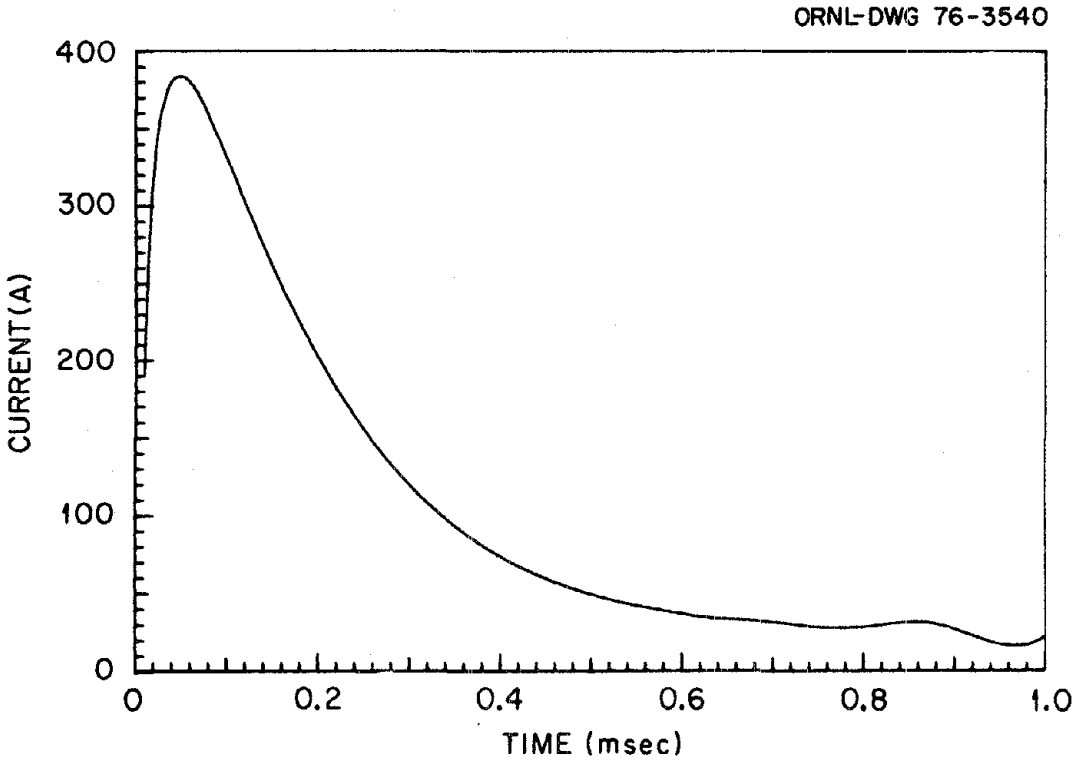

(*a*) EARLY TIME CONDUIT CURRENT

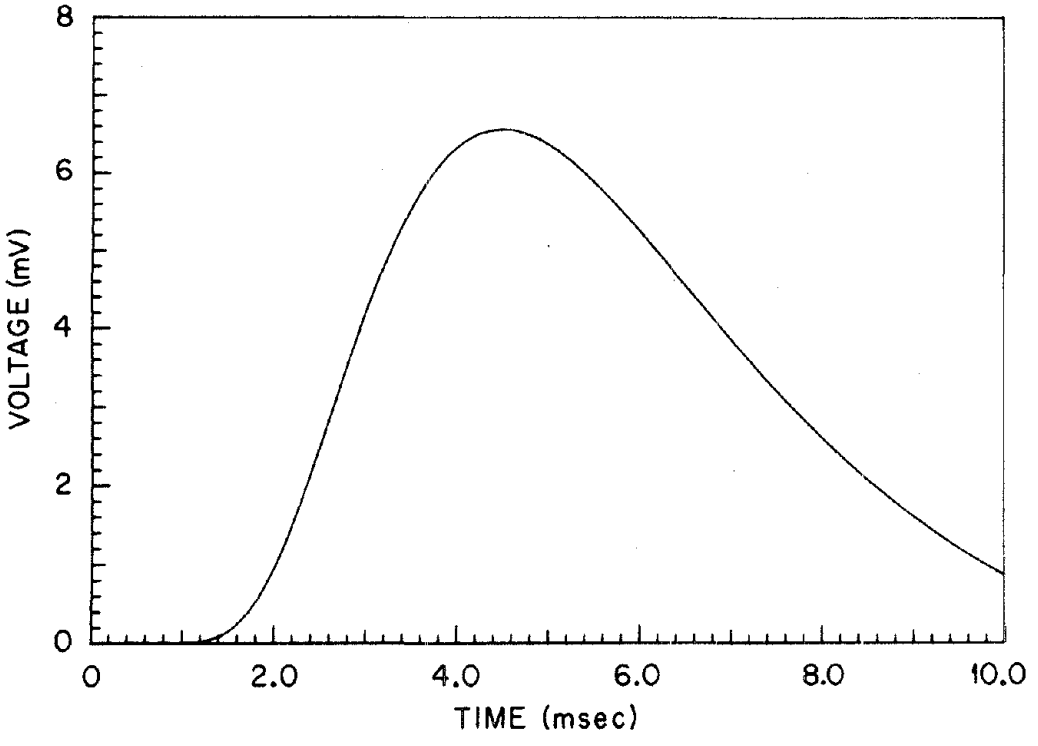

(*b*) OPEN CIRCUIT VOLTAGE BETWEEN CONDUIT AND INTERNAL CABLE

Fig. 4.1. Surges Induced on a 160 m Conduit Located 10 m Above the Earth by the Representative EMP with $\theta = 80^{o}$, $\psi = 60^{o}$, and $\phi = 180^{o}$.

The voltage coupled to a conductor inside the conduit is shown in Fig. 4.1b. The peak voltage of 6.6 mV, coupled to the internal conductor by diffusion, compares well with that obtained experimentally.[7] The measured peak voltage induced on a conductor in a 3.05 m (10-ft) conduit due to a current pulse with a 150 A peak is 68 μV. The experimental transfer impedance can be calculated from Eq. (3.9) as 0.149 μV/A-m. For a 390 A peak conduit current and ℓ equal to 160 m, the substitution of the experimental transfer impedance into Eq. (3.9) gives a peak induced voltage of 9.28 mV. The relative difference between the measured and calculated values is 29%.

The leakage signal coupled through breaks in the conduit occur at couplings, pull boxes, junction boxes, flexible conduit, and unions. Normally, the leakage signal is larger than the diffusion signal. The leakage signal is a function of the contact made by the threaded connections. Improperly tightened threads or rusty threads increase the surge coupled by leakage.

In Ref. 6, the leakage signal of 36 mV, coupled through a wrench-tight coupling in the center of a 3.05 m (10-ft) conduit section, was measured (see Test 4a). For comparison, a hand-tight coupling induced 1.08 V (see Test 1d). The conduit current had a 150 A peak, a 3 nsec rise time, and a 4 μsec (e-fold) fall time.

The leakage inductance can be computed by

$$M = \frac{V_{oc}}{\ell\left(\frac{d\ I_s}{d_t}\right)} \quad . \tag{4.2}$$

In the experiment, ℓ = 3.05 m and $d\ I_s/d_t$ initially was equal to about 5×10^{10} A/sec. The value of M for a wrench-tight coupling is 0.23 pH/m, where one coupling is used for every 3.05 m length of conduit.

For the 160 m line that we have used as a model, $d\ I_s/d_t \simeq 2 \times 10^{10}$ A/sec. The open circuit voltage induced is 0.76 V. The characteristic impedance for the conduit-internal wire transmission line is about 100 Ω; thus, the short circuit current peak is roughly 7 mA.

The current induced on the conductor inside the conduit has an initial spike of 7 mA with about twice the rate of rise as the conduit current. This initial spike drops to near zero when the shield current reaches its peak value. Later, the peak current coupled by diffusion is only about 60 μA. If the internal conductor in the conduit is the shield of a coaxial cable, the short circuit current from the internal coax conductor to the cable shield will rise to about 8 μA and then decrease to a damped oscillating current with an initial peak near 1.0 μA. Double-shielded cables such as triaxial cables will attenuate the initial spike, and the late-time surge will be reduced to about 0.5 μA.

It should be pointed out that if a shielded cable in a conduit is grounded at both ends much of the shielding benefits at late times ($t > 2\ell/c$) of the conduit are lost. The current surge will divide between the cable shield and the conduit, since they are both grounded at each end. About 3.3% of the current induced in a 2-in. conduit will flow in the shield of an RG-59B coaxial cable. However, the conduit system which is grounded at both ends of the 160 m line will couple a current surge with a peak three times larger than that of a single-grounded line. Thus, the late-time shield current of a cable grounded at both ends in conduit is one-tenth that of the single-grounded cable not protected by conduit.

4.3 Cable Trays

Cables in cable trays can benefit from the shielding effects of a cable bundle. The cables on the outside of the bundle tend to shield the internal cables. Also, the cables on the outside of the bundle tend to share the current that would be induced in an equivalent conductor with an effective radius of the cable bundle. The induced current is not a strong function of radius. The peak current is proportional to a logarithmic function of the radius.[8]

For a cable bundle with an effective radius equal to 0.17 m, consisting of cables with radii equal to 3.25 mm, the bulk cable current is only about 50% larger than the current induced on a single cable. The number of cables in a tray ranges from about fifty to several hundred. For a cable bundle consisting of 50 cables, nearly 20 cables will be located in the outside of the bundle. The current induced in each

outside cable will be about 7.5% of the current induced in a single cable. For a large bundle with a rectangular cross section consisting of 300 cables, about 100 cables may be located on the outside of the bundle. The current induced in each outside cable will be about 1.5% of the current induced in a single cable. Thus, the shielding effectiveness of cable bundles in nuclear plants ranges from about 22 dB to 36 dB.

The cables are generally randomly located in the cable bundle. A particular cable is equally likely to be at any position in the bundle cross section and is equally likely to be at any other position in the bundle at any other position along the cable bundle. Because of the random positions of the cables, the shielding effectiveness for the outer cables is assigned to all of the cables.

4.4 The Building Interior

The EMP electric and magnetic fields are attenuated by the building structural members such as steel beams, rebar construction, and poured-in-place concrete. The shielding effectiveness of the building increases for positions toward the center of the building. The magnetic shielding effectiveness due to the rebar construction in the exterior walls is about 20 dB greater at the center of the building than it is a few feet from the wall.[2]

The electric field shielding effectiveness of the Sequoyah nuclear plant control building was measured for broadcast band AM and FM signals by ORNL. The shielding effectiveness in the center of the building on the bottom floor is at least 20 dB greater than it is on the top floor. This is an estimated value since the actual signal was at the noise level of the plant. A conservative estimate of the additional EMP shielding for cables located deep in the building interior is 20 dB.

5. SUMMARY

In this report, the electrical surges induced in nuclear power plant cables by a high-altitude nuclear electromagnetic pulse have been considered. Two EMP incident directions have been used in the calculations, broadside incidence ($\theta = 80^{o}$, $\psi = 90^{o}$, and $\phi = 90^{o}$) and along-the-line incidence ($\theta = 80^{o}$, $\psi = 60^{o}$, and $\phi = 180^{o}$). Both incident directions were chosen for a high-altitude nuclear detonation far from the plant such that the EMP source appears to be located just above the horizon. It was found that broadside incidence induces the largest response for short cables on the order of 20 m, and along-the-line incidence results in the largest response for long cables on the order of 160 m.

The magnitude and duration of the EMP surges depend on many parameters. The properties of some EMP surges induced in cables of different lengths and various effective shielding levels are summarized in Table 5.1.

The EMP direction of incidence that resulted in the largest response was used to construct the table. Some important parameters that determine the amplitude and duration of an EMP surge coupled to a cable are: (1) the shielding effectiveness of the building, (2) the location of the cable within the building, (3) the type and length of the cable, (4) the direction of the incident EMP with respect to the cable and the earth, and (5) the time history of the EMP waveform. The effects of conditions 1, 2, and part of 3 above have been studied to a limited degree in this report.

The results of this study are more accurate for unshielded lines than for shielded lines. As the shielding level of the cable is increased, the problem becomes more complex, and the accuracy is normally decreased. The shielding effects of the walls, conduits, cable shields, cable trays, etc. have been approximated by functions that result in slightly higher EMP energies coupled to the cable. Therefore, the EMP surges presented in this report are useful for a vulnerability analysis of severe EMP surges on nuclear power plants.

Table 5.1 Summary of EMP Cable Surges

Cable	Location	V_p	ROR	Duration (μsec)	I_p
20 m Copper Wire	Near an external wall	26 kV	1.47 kV/ns	0.5	52 A
20 m Copper Wire	Deep within the building	2.6 kV	147 V/ns	0.5	5.2 A
160 m Copper Wire	Near an external wall	88 kV	7.12 kV/ns	6.4	170 A
160 m Copper Wire	Deep within the building	8.8 kV	710 V/ns	6.4	17 A
160 m Copper Wire	Near an external wall in a cable tray	8.8 kV	710 V/ns	6.4	17 A
160 m RG-59B Coaxial Cable	Near an external wall	80 V	1.0 V/ns	50	2.2 A
160 m RG-59B Coaxial Cable	Near an external wall in conduit	0.6 mV	0.2 mV/ns	10 ms	8 μA
160 m Triaxial Cable	Near an external wall	44 V	0.38 V/ns	50	1.4 A
160 m Triaxial Cable	Near an external wall in conduit	37.5 μV	15.6 μV/ns	10 ms	0.5 μA
160 m Shielded Twisted Pair	Near an external wall	8 V	100 mV/ns	50	220 mA
160 m Shielded Twisted Pair	Near an external wall in a cable tray	0.8 V	10 mV/ns	50	22 mA

V_p = Peak open circuit voltage. ROR = Initial rate of rise from 10-90% of the open circuit voltage.

I_p = Peak short circuit current. Duration = Time that the voltage surge has decreased to 10% of V_p.

APPENDIX A

CALCULATED EMP SURGES ON UNSHIELDED LINES

CALCULATED EMP SURGES ON UNSHIELDED LINES

The following figures show the short circuit current and open circuit voltage surges induced in unshielded copper lines located 10 m above a finitely conducting earth. The radius of the wire is 3.25 mm, and the earth conductivity is 5 mℑ/m. The geometry of the EMP-line interaction problem is shown in Fig. 2.1b. For finite length lines, the source end of the line ($y = -\ell$) is terminated by an open circuit.

The representative EMP electric field time history selected for the calculations is given by Eq. (1.1) with $E_o = 5.3$ kV/m, $\alpha = 5 \times 10^6$ sec^{-1}, and $\beta = 5 \times 10^8$ sec^{-1}. The source of the representative EMP is located at 10^o above the horizon ($\theta = 80^o$). Two EMP incident directions have been selected; one is broadside to the wire ($\phi = 90^o$) and the other is in the plane formed by the y-z axis.

A list of the figures that follow is given below.

Figure No.	Caption
A1	Surges induced on a semi-infinite line located 10 m above the earth by the representative EMP with $\theta = 80^o$, $\psi = 60^o$, and $\phi = 180^o$.
A2	Surges induced on a semi-infinite line located 10 m above the earth by the representative EMP with $\theta = 80^o$, $\psi = 60^o$, and $\phi = 0^o$.
A3	Surges induced on a 160 m line located 10 m above the earth by the representative EMP with $\theta = 80^o$, $\psi = 60^o$, and $\phi = 180^o$.
A4	Surges induced on a 160 m line located 10 m above the earth by the representative EMP with $\theta = 80^o$, $\psi = 90^o$, and $\phi = 90^o$.
A5	Surges induced on a 20 m line located 10 m above the earth by the representative EMP with $\theta = 80^o$, $\psi = 90^o$, and $\phi = 90^o$.
A6	Surges induced on a 20 m line located 10 m above the earth by the representative EMP with $\theta = 80^o$, $\psi = 60^o$, and $\phi = 180^o$.

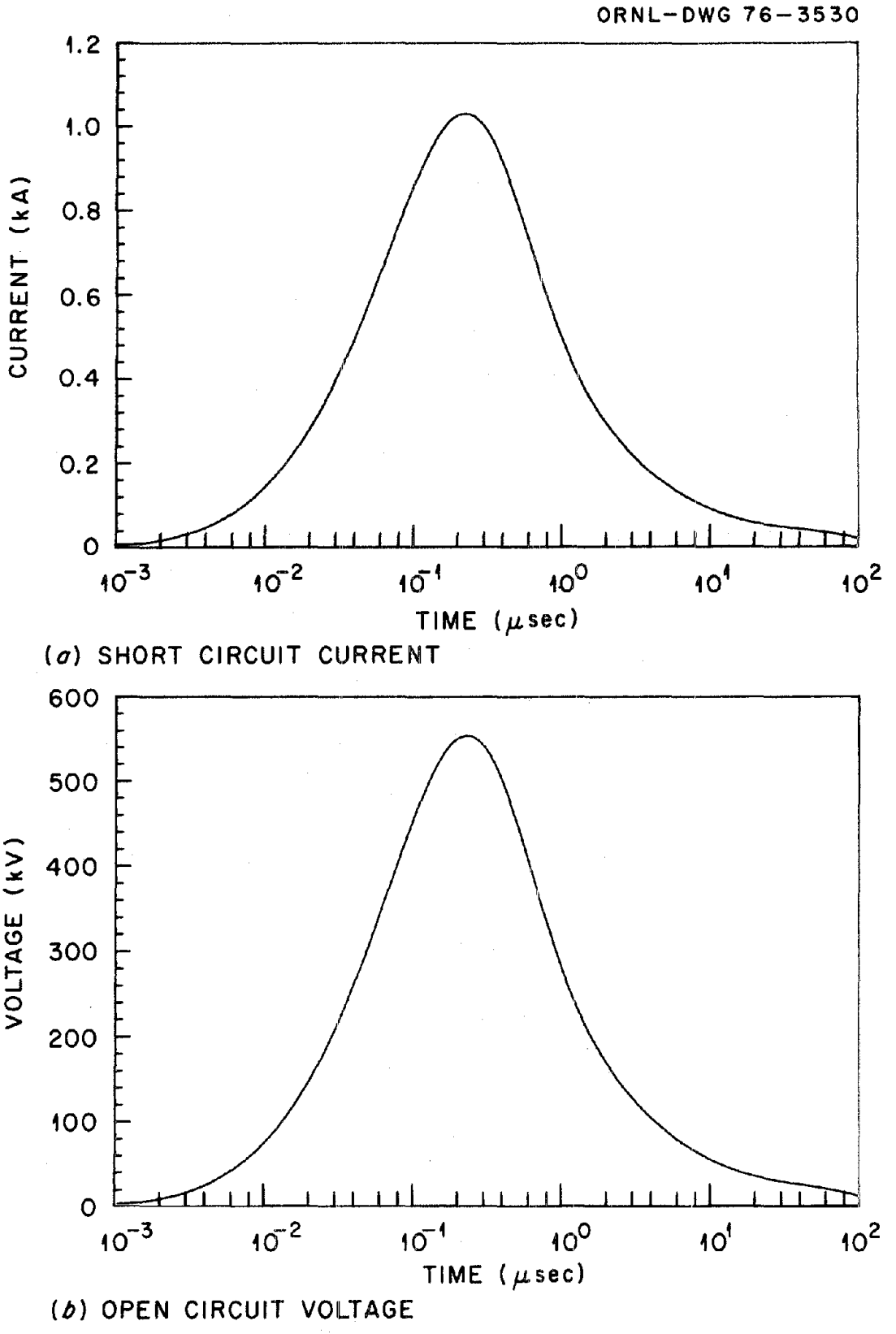

Fig. A1. Surges Induced on a Semi-Infinite Line Located 10 m Above the Earth by the Representative EMP with $\theta = 80^{\circ}$, $\psi = 60^{\circ}$, and $\phi = 180^{\circ}$.

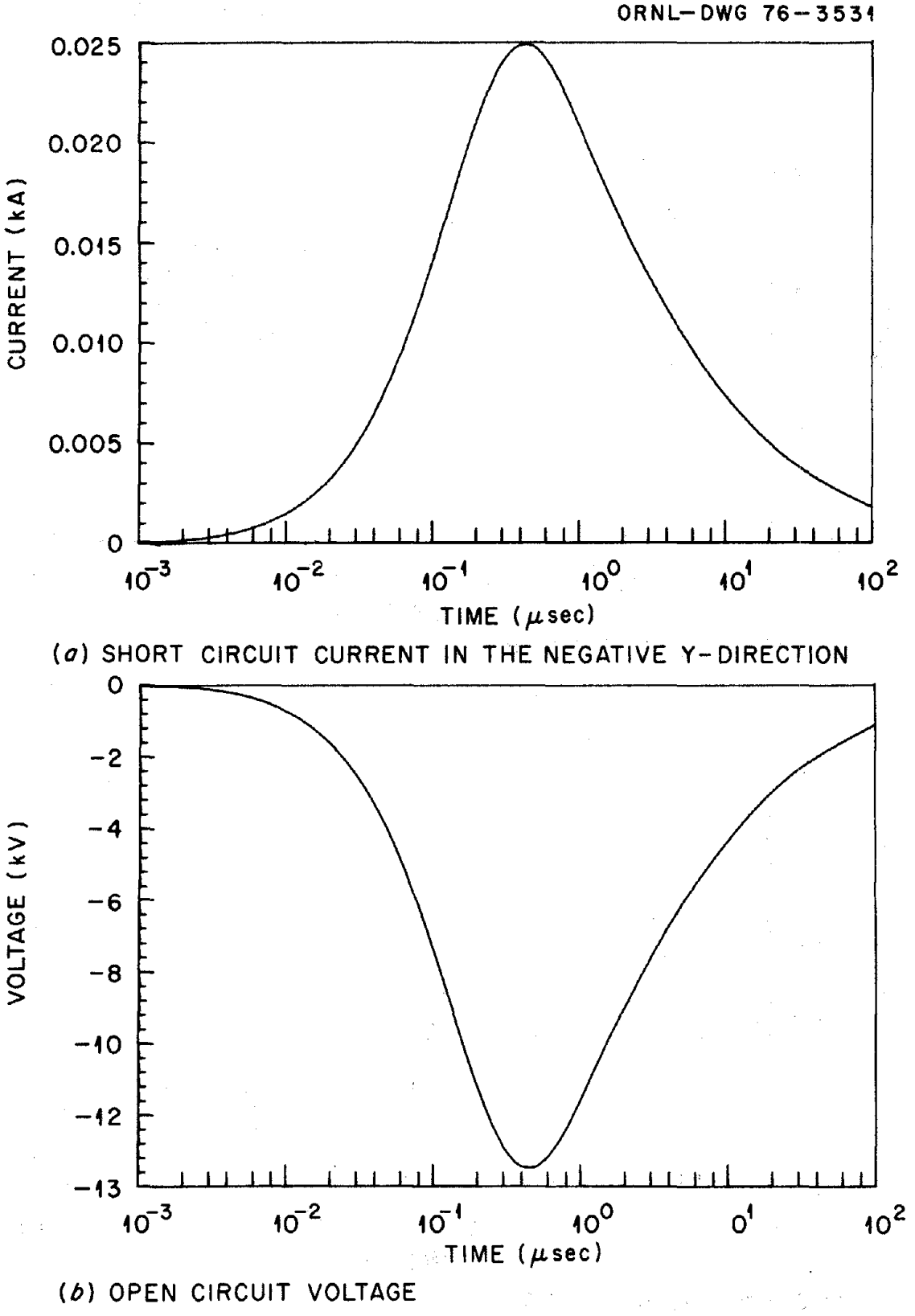

Fig. A2. Surges Induced on a Semi-Infinite Line Located 10 m Above the Earth by the Representative EMP with $\theta = 80^{o}$, $\psi = 60^{o}$, and $\phi = 0^{o}$.

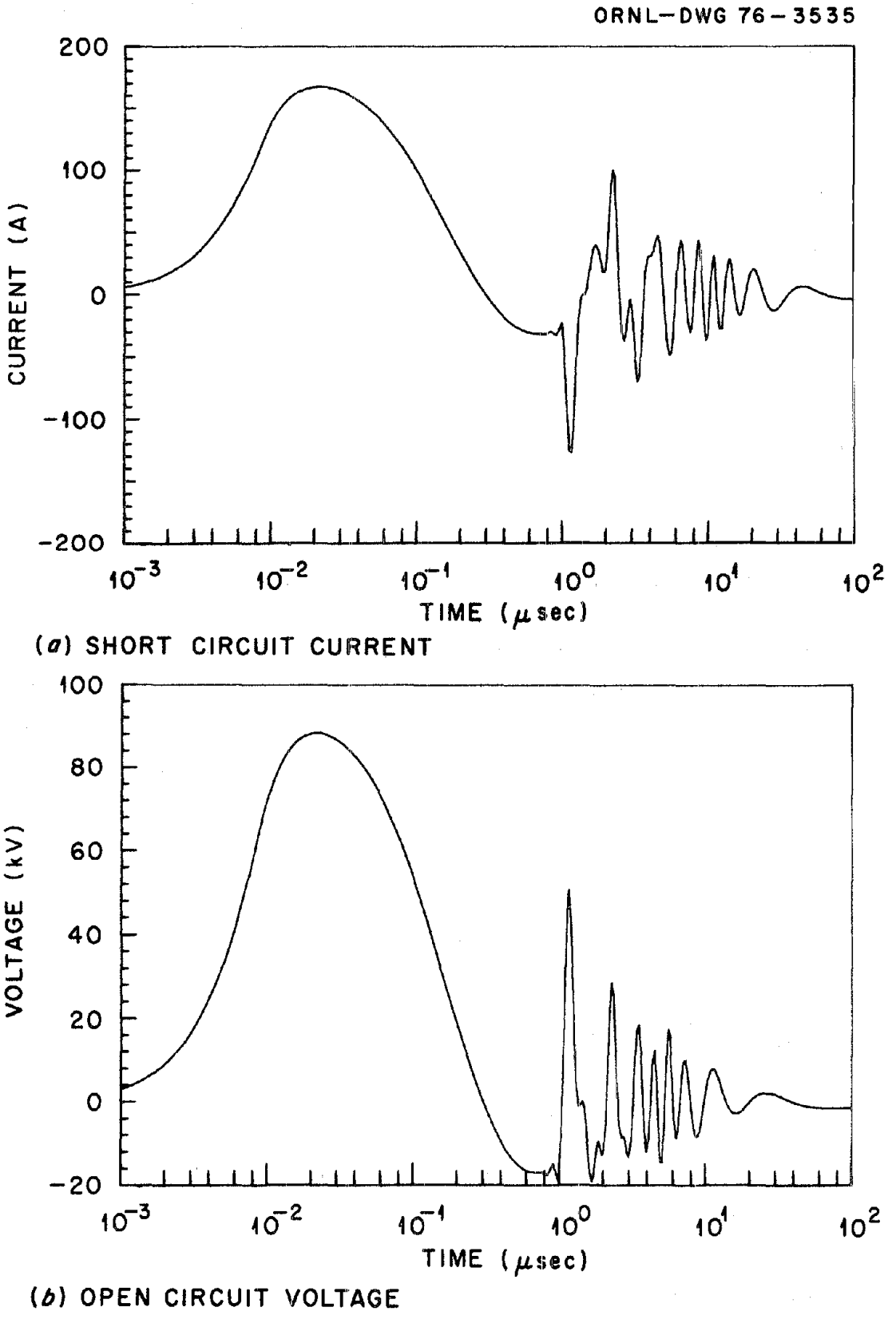

Fig. A3. Surges Induced on a 160 m Line Located 10 m Above the Earth by the Representative EMP with $\theta = 80^{\circ}$, $\psi = 60^{\circ}$, and $\phi = 180^{\circ}$.

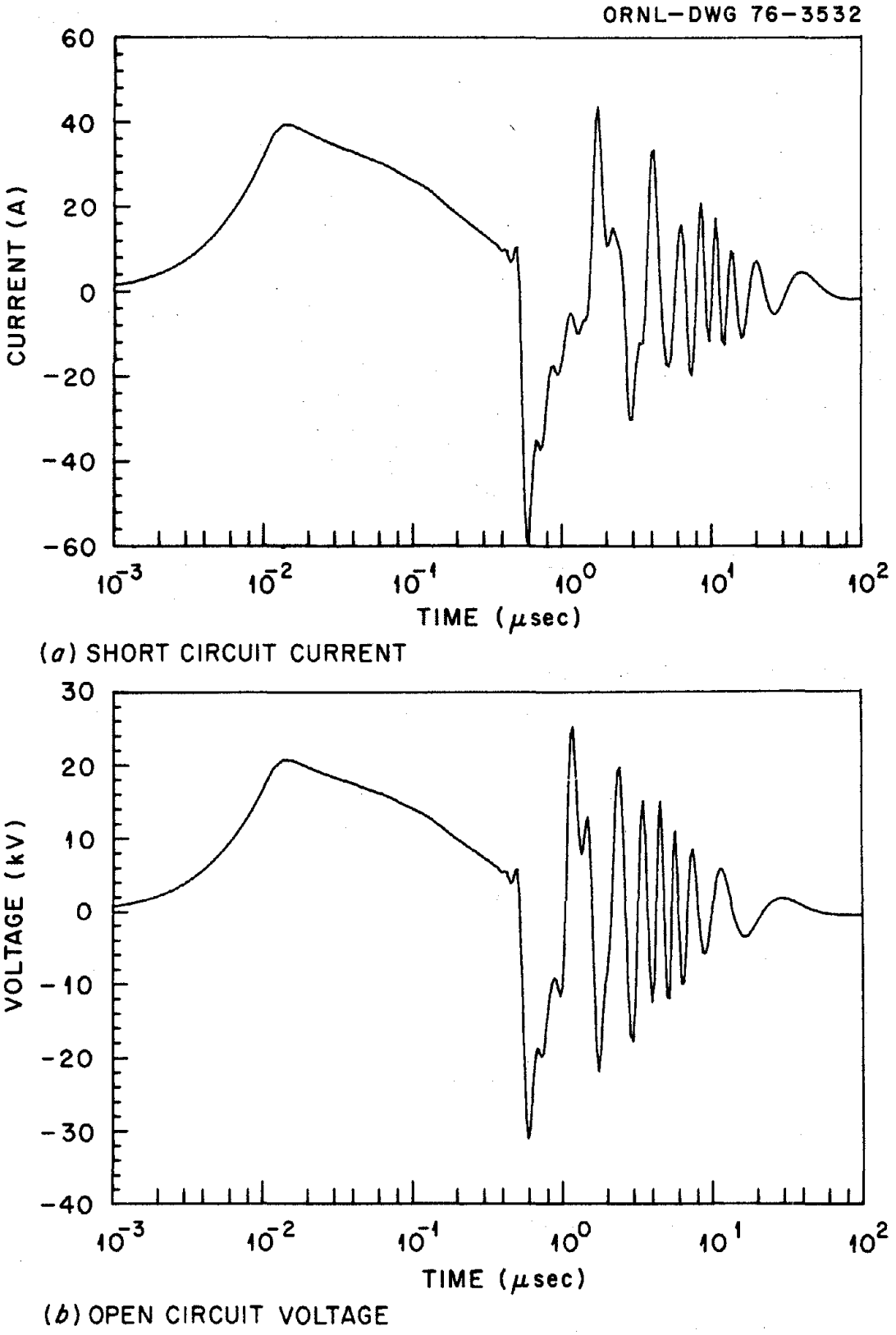

Fig. A4. Surges Induced on a 160 m Line Located 10 m Above the Earth by the Representative EMP with $\theta = 80^{\circ}$, $\psi = 90^{\circ}$, and $\phi = 90^{\circ}$.

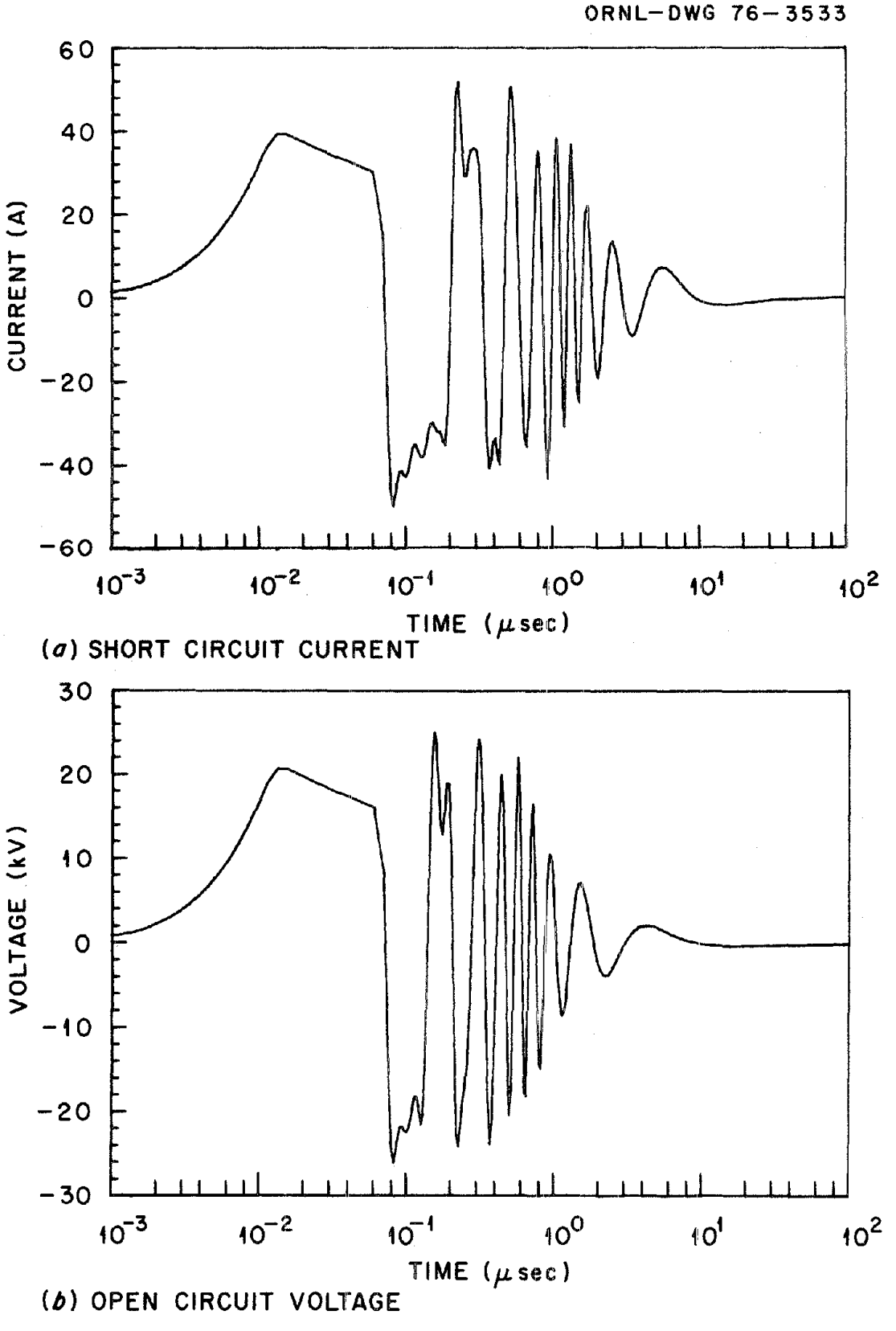

Fig. A5. Surges Induced on a 20 m Line Located 10 m Above the Earth by the Representative EMP with $\theta = 80^{o}$, $\psi = 90^{o}$, and $\phi = 90^{o}$.

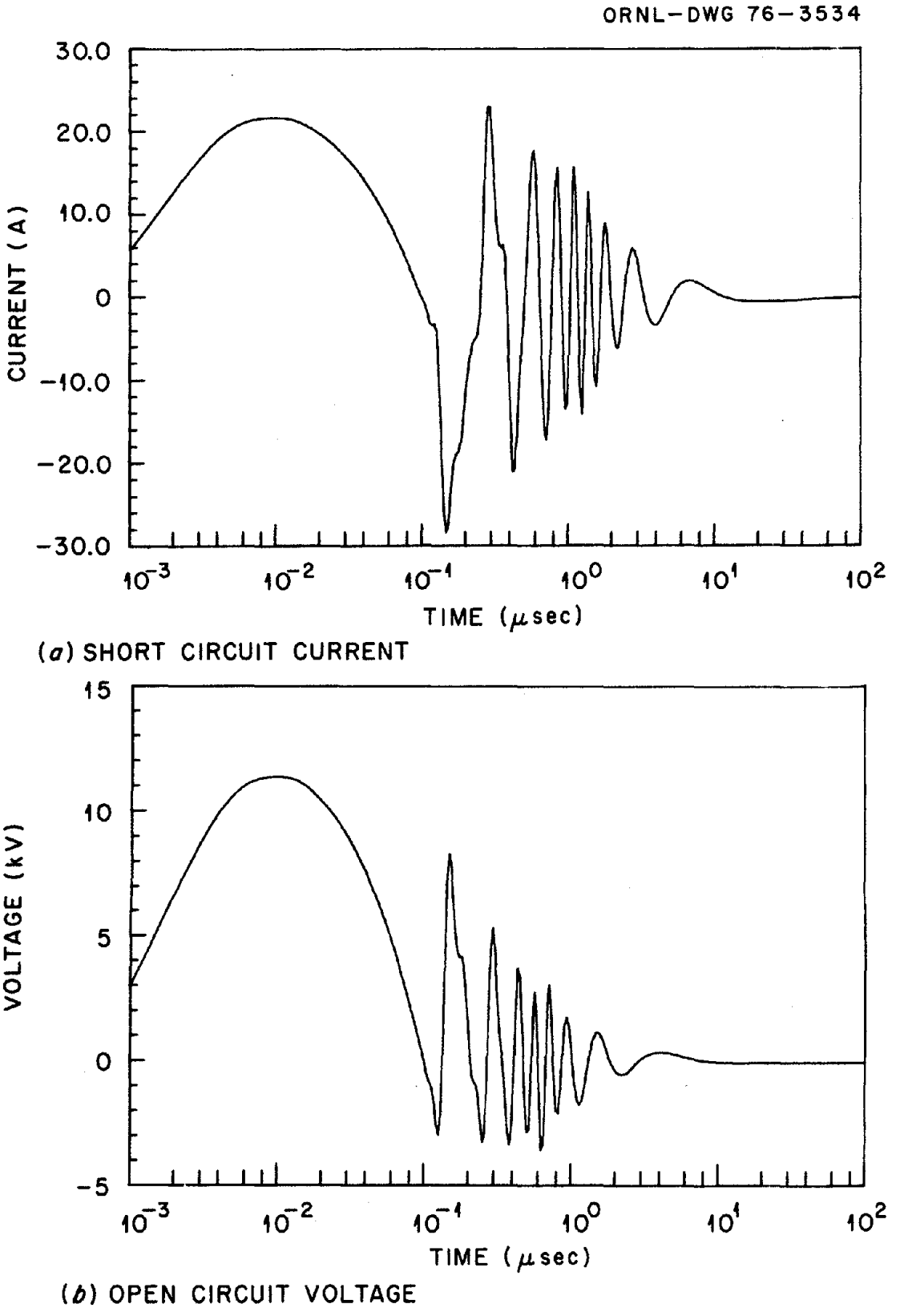

Fig. A6. Surges Induced on a 20 m Line Located 10 m Above the Earth by the Representative EMP with $\theta = 80^{\circ}$, $\psi = 60^{\circ}$, and $\phi = 180^{\circ}$.

APPENDIX B

CALCULATED BRAIDED, SHIELDED CABLE RESPONSES

CALCULATED BRAIDED, SHIELDED CABLE RESPONSES

The following four figures show the EMP surges induced in coaxial and triaxial cables located 10 m above the earth by the representative EMP at broadside incidence.

A list of figures follows below.

Figure No.	Caption
B1	Surges induced in a semi-infinite coaxial cable similar to RG-59B located 10 m above the earth by the representative EMP with $\theta = 80^{o}$, $\psi = 90^{o}$, and $\phi = 90^{o}$.
B2	Surges induced on a semi-infinite triaxial line located 10 m above the earth by the representative EMP with $\theta = 80^{o}$, $\psi = 90^{o}$, and $\phi = 90^{o}$.
B3	Surges induced in a 160 m coaxial cable similar to RG-59B located 10 m above the earth by the representative EMP with $\theta = 80^{o}$, $\psi = 90^{o}$, and $\phi = 90^{o}$.
B4	Surges induced in a 160 m triaxial cable located 10 m above the earth by the representative EMP with $\theta = 80^{o}$, $\psi = 90^{o}$, and $\phi = 90^{o}$.

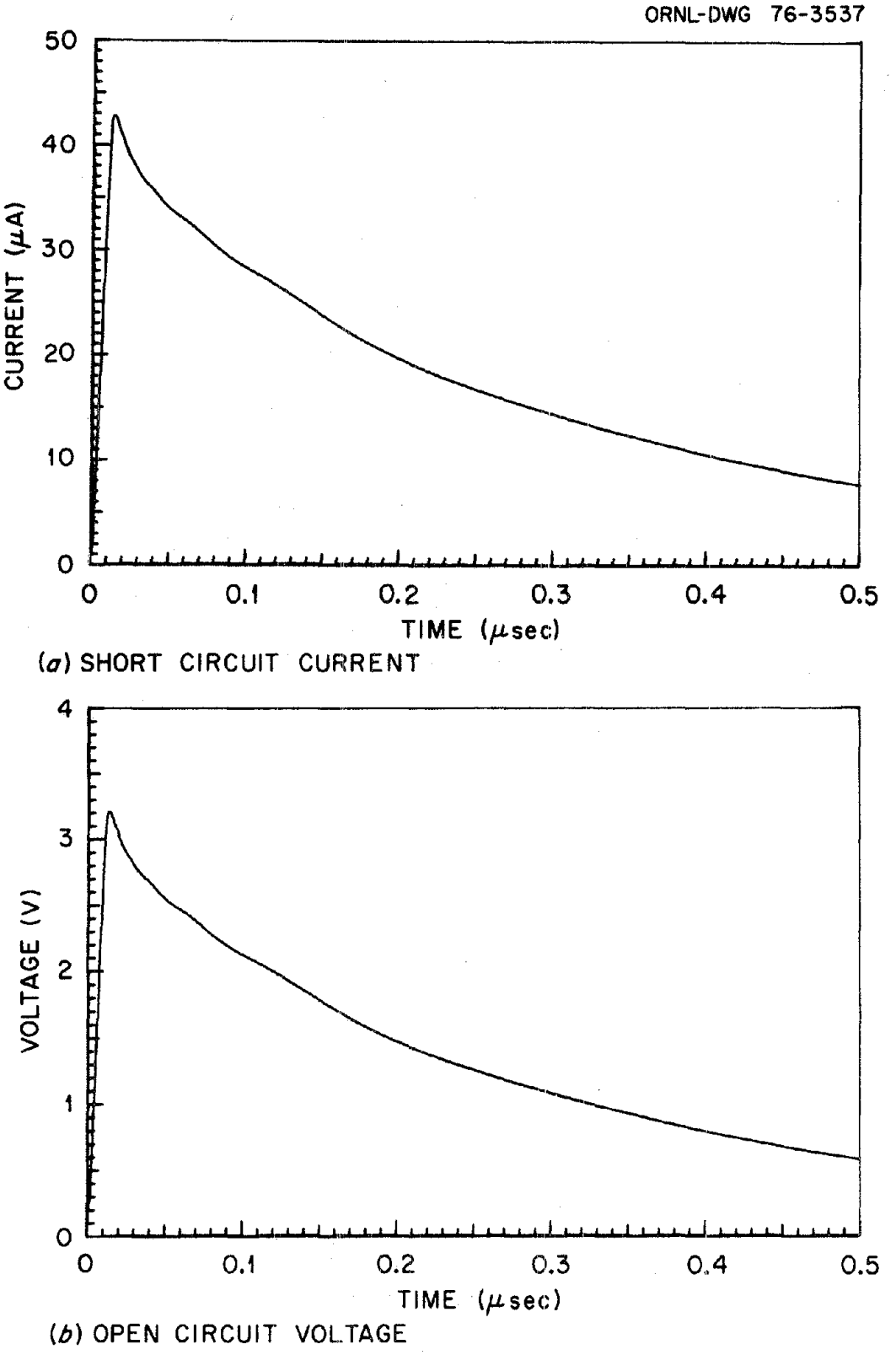

Fig. B1. Surges Induced in a Semi-Infinite Coaxial Cable Similar to RG-59B Located 10 m Above the Earth by the Representative EMP with $\theta = 80^{\circ}$, $\psi = 90^{\circ}$, and $\phi = 90^{\circ}$.

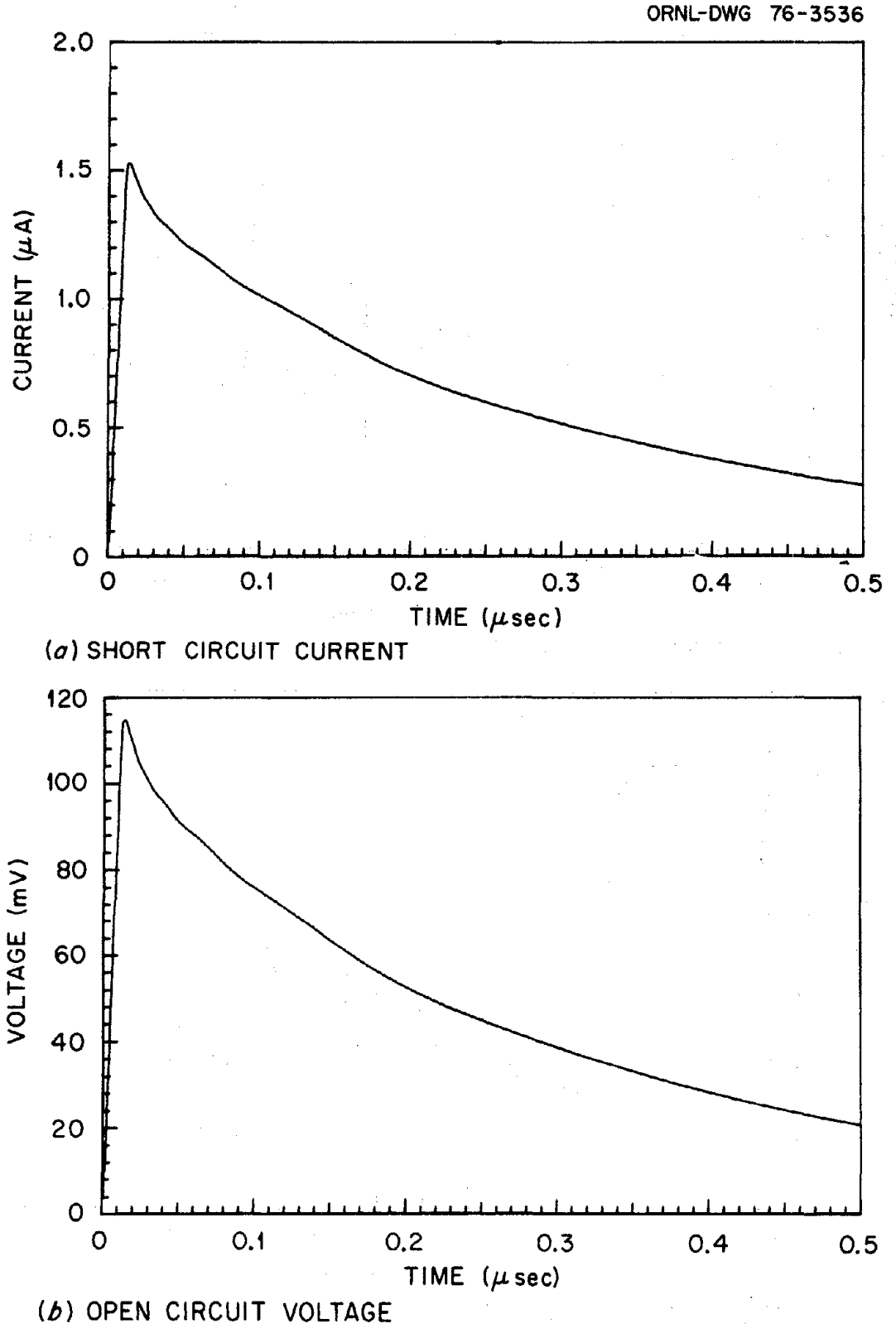

Fig. B2. Surges Induced on a Semi-Infinite Triaxial Line Located 10 m Above the Earth by the Representative EMP with $\theta = 80^{\circ}$, $\psi = 90^{\circ}$, and $\phi = 90^{\circ}$.

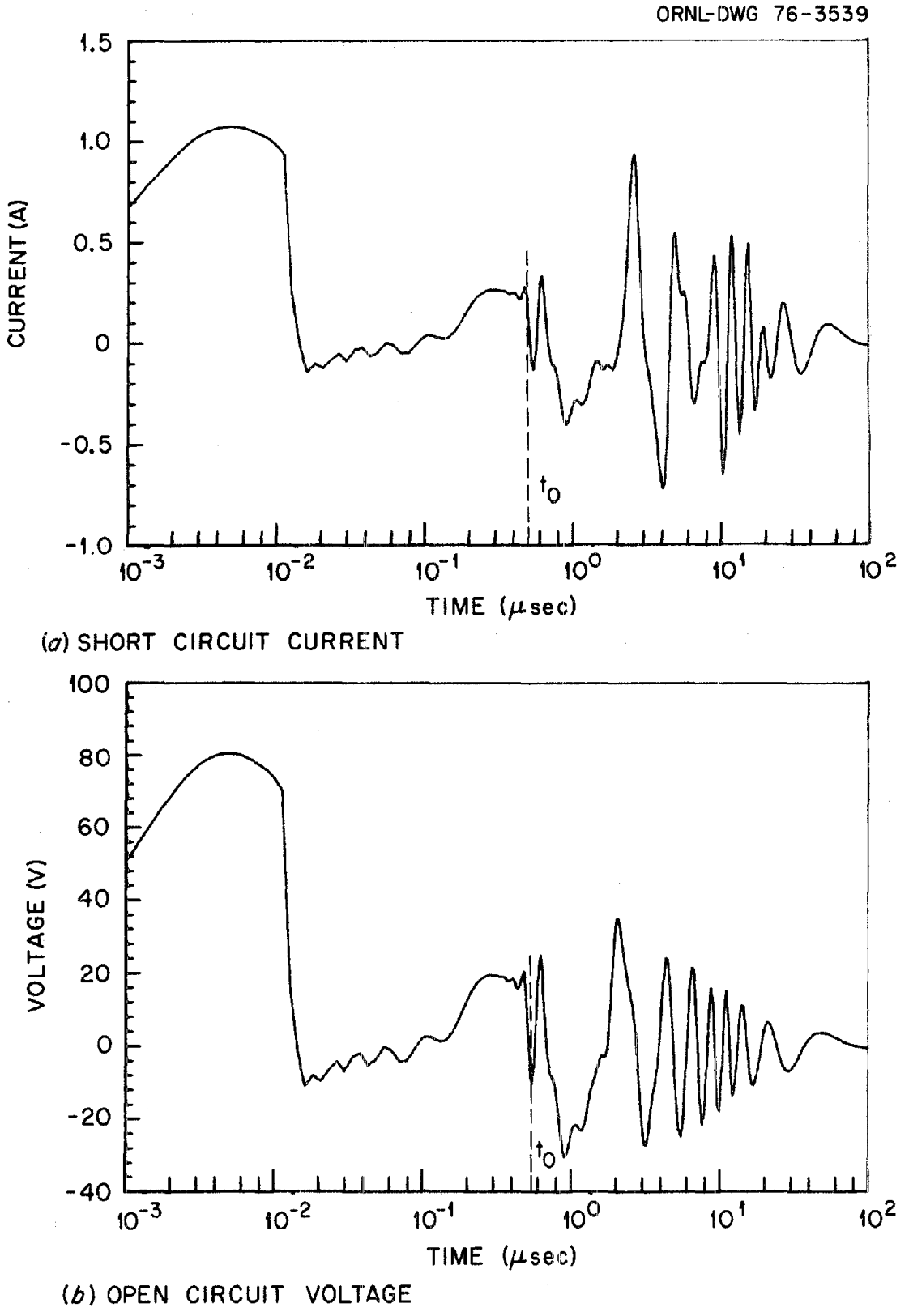

Fig. B3. Surges Induced in a 160 m Coaxial Cable Similar to RG-59B Located 10 m Above the Earth by the Representative EMP with $\theta = 80^{\circ}$, $\psi = 90^{\circ}$, and $\phi = 90^{\circ}$.

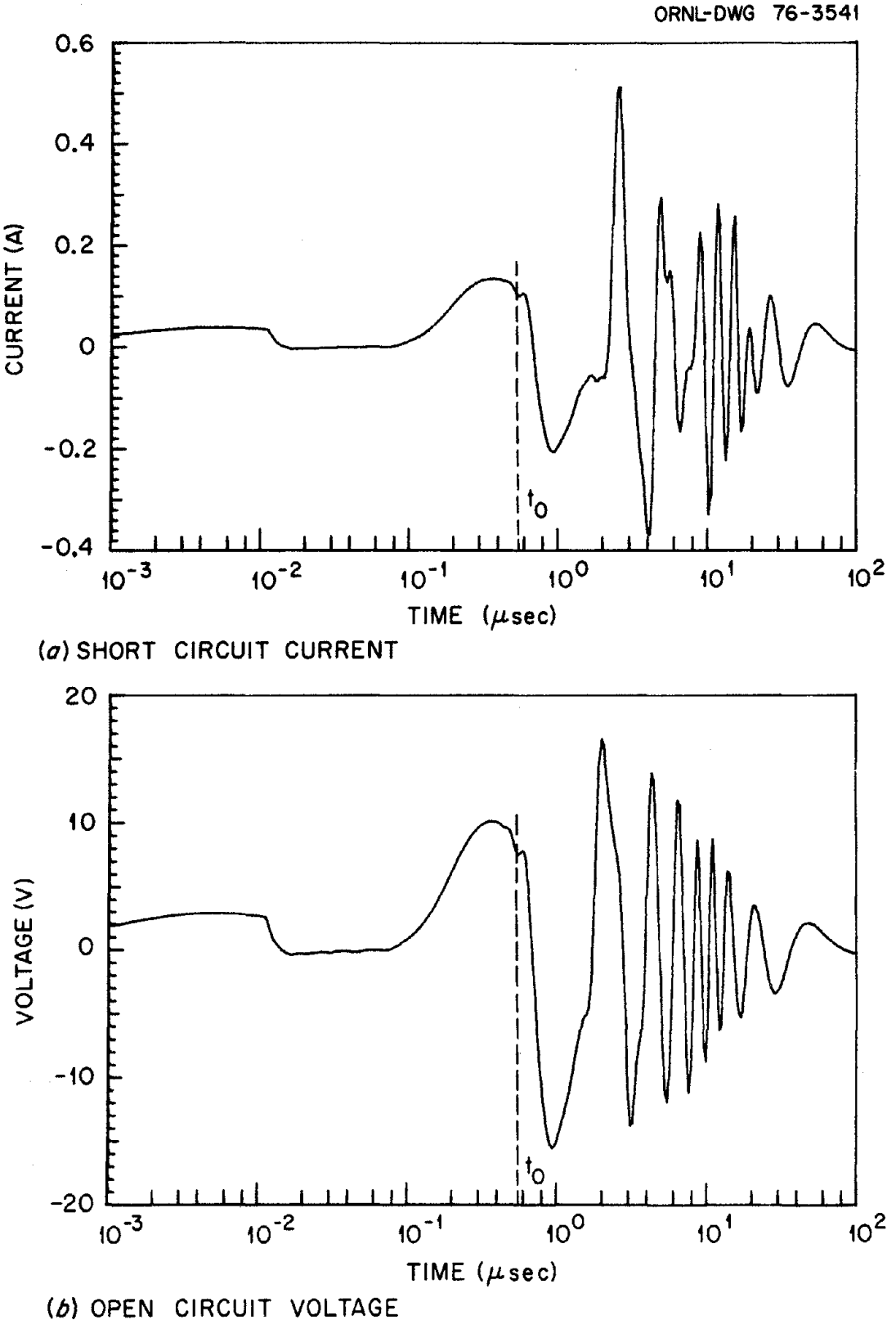

Fig. B4. Surges Induced in a 160 m Triaxial Cable Located 10 m Above the Earth by the Representative EMP with $\theta = 80^{\circ}$, $\psi = 90^{\circ}$, and $\phi = 90^{\circ}$.

REFERENCES

1. J. H. Marable, P. R. Barnes, and D. B. Nelson, Power System EMP Protection, ORNL-4958, Oak Ridge National Laboratory, Oak Ridge, Tennessee, March 1975.
2. R. Sherman et al., EMP Engineering and Design Principles, Bell Laboratories, 1975.
3. E. F. Vance, "Coupling to Cables," DNA Handbook Revision, Chapter 11, December 1974.
4. E. D. Knowles and L. W. Olson, Cable Shielding Effectiveness Testing, PEM-14, Lawrence Livermore Laboratory, Livermore, California.
5. J. C. Erb, Cable Coupling and Shielding Model, PEM-11, Lawrence Livermore Laboratory, Livermore, California.
6. G. L. Brown, Shielding Evaluation of Braided Cable Sheaths and Multiconductor Cables Using Pulse Test Methods, PEM-13, Lawrence Livermore Laboratory, Livermore, California, August 1974.
7. D. J. Leverenz, P. H. Nielsen, and R. G. McCormack, EMP Shielding Properties of Conduit Systems and Related Hardware, Technical Report C-19, Construction Engineering Research Laboratory, Champaign, Illinois, June 1975.
8. P. R. Barnes, The Axial Current Induced on an Infinitely Long, Perfectly Conducting, Circular Cylinder in Free Space by a Transient Electromagnetic Plane Wave, Interaction Note 64, Air Force Weapons Laboratory, Kirtland AFB, New Mexico, March 1971.